Stony Brook University

The Role of TRAF4 within BMP Signaling and the Developing Ectoderm

A Dissertation Presented

by

Francesca Marie Gist Nakagawa

to

The Graduate School

in Partial Fulfillment of the Requirements

for the Degree of

Doctor of Philosophy

in

Molecular and Cellular Pharmacology

Stony Brook University

August 2015

Stony Brook University

The Graduate School

Francesca Marie Gist

We, the dissertation committee for the above candidate for the Doctor of Philosophy degree, hereby recommend acceptance of this dissertation.

Gerald H. Thomsen, Ph.D. – Dissertation Advisor

Professor, Department of Biochemistry and Cell Biology

Ken-Ichi Takemaru, Ph.D. – Chairperson of Defense

Associate Professor, Department of Pharmacological Sciences

David Talmage, Ph.D. – Committee Member

Professor, Department of Pharmacological Sciences

Peter Gergen, Ph.D. – Outside Member

Professor, Department of Biochemistry and Cell Biology

This dissertation is accepted by the Graduate School

Charles Taber

Dean of the Graduate School

Abstract of the Dissertation

The Role of TRAF4 within BMP Signaling and the Development of the Ectoderm

by

Francesca Marie Gist Nakagawa

Doctor of Philosophy

in

Molecular and Cellular Pharmacology

Stony Brook University

2015

TGF-β signaling is essential for the induction and patterning of the early embryonic germ layers. Within TGF-β signaling, regulation of BMP signaling is necessary for patterning the ectoderm, where ventrally located BMPs induce epidermis, and dorsally located BMP inhibitors allow for neural induction. In *Xenopus laevis*, this sensitivity of the ectoderm to BMP signaling allows for the differentiation of the presumptive ectoderm to be used as a readout of BMP activity. Increased BMP signaling expands epidermal tissue, and decreased BMP signaling results in an expansion of neural tissue. Tumor Necrosis Factor-Receptor Associated Factor 4 (TRAF4), is an adaptor protein with functions in ontogenic processes, adult epithelial progenitor cells and cancer metastasis. TRAF4 has been shown to potentiate BMP signaling, but the extent of TRAF4 involvement in the BMP pathway and the fate of the ectoderm are not well understood. In this study, I show that TRAF4 is needed for the differentiation of the epidermis and that TRAF4 is needed for robust BMP signaling to occur.

TRAF4 is expressed in the presumptive ectoderm of the early embryo, and enveloping ectoderm of the gastrula. At neurula stages, TRAF4 becomes restricted to dorso-anterior and neural tissue. TRAF4 knockdown in *Xenopus laevis* embryos results in incomplete gastrulation and a loss of anterior structures. Consistent with its expression pattern in the ectoderm, TRAF4 knockdown results in the loss of epidermal differentiation, and the ectoderm trends towards

neural differentiation, suggesting that the presence of TRAF4 is needed for epidermal differentiation. In addition, embryos that overexpress BMP4 fail to gastrulate, yet knockdown of TRAF4 results in embryos that regain the ability to perform gastrulation movements. These data suggest that TRAF4 is positively regulating BMP signaling, and that TRAF4 is needed for proper gastrulation, and differentiation of the epidermis.

Dedication Page

To my family and friends, for believing in me.

To that guy from Osaka, for following me across the Northern Hemisphere, and supporting my decisions without a second thought.

To Bianca, for waking me up to the fact that I can do more.

Frontispiece

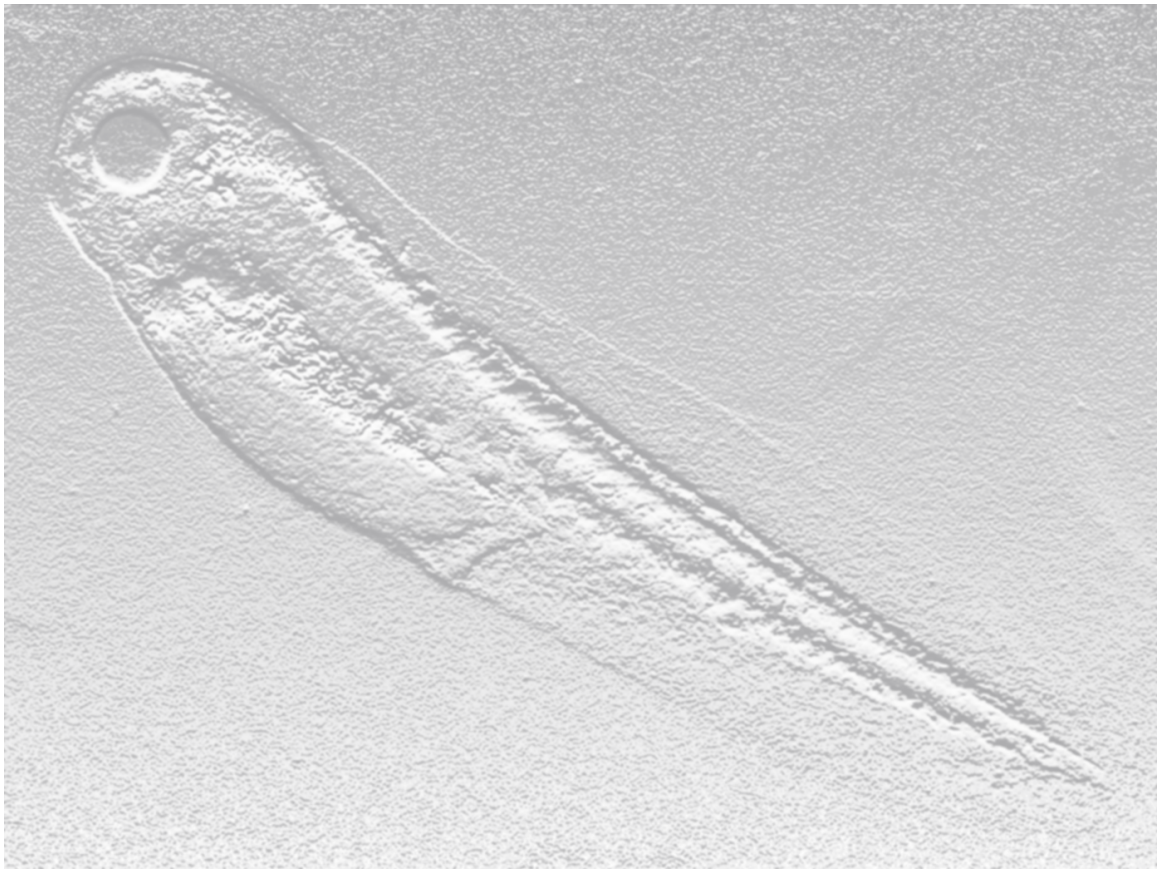

Table of Contents

List of Figures

List of Tables

List of Abbreviations

A-P:	Anterior-Posterior
Bra:	Brachyury
BMP:	Bone Morphogenetic Protein
BMP4:	Bone Morphogenetic Protein 4
Cer:	Cerberus
Chd:	Chordin
Gsc:	Goosecoid
MO:	Morpholino
NCAM:	Neural Cell Adhesion Molecule
ORF:	Open Reading Frame
R-Smad:	Receptor-Smad
RT-PCR:	Real Time Polymerase Chain Reaction
SMURF:	Smad Ubiquitination Regulatory Factor
TRAF4:	Tumor Necrosis Factor-Receptor Associated Factor 4
UTR:	Untranslated Region
XAG-1:	Xenopus Anterior Gradient-1
Xnr2:	Xenopus Nodal-related 2

Acknowledgments

I would like to thank my advisor and mentor Gerald H. Thomsen. I was immediately attracted to Jerry's lab by his enthusiasm and excitement for science. Without Jerry's belief in my abilities, I may not have seen my doctoral studies to their completion. I thank Jerry for the opportunities and growth graduate studies in science research have given me and look forward to seeing Jerry in the future.

I would like to thank my committee chair Ken-Ichi Takemaru for his steadfast confidence in my abilities and sincere interest in my work. His insightful questions taught me much about analyzing and understanding scientific inquiry.

I would like to thank my committee member David Talmage for his kindness, belief in my abilities and straight answers to my questions. David had every confidence that I could complete any experiment I suggested. I want to thank him for creating a welcoming environment where any question could be asked.

I would like to thank my outside committee member Peter Gergen for treating me as an intellectual equal and sharing his thoughts and ideas. Peter had every confidence that I could understand and incorporate his input, and I greatly appreciate that he respected my intellectual abilities enough to never hold his feelings back. His insight and experience has pushed me to think as a scientist, a skill that requires mentorship to grow.

I would like to thank my present and former lab-mates Lidia Sobkow, William Gillis, Matthew Dunn, Gina Sorrentino, Donghyuk Ki, and Jamina Oomen-Hajagos. They have all given me protocols, explained procedures and gone out of their way to teach me what they know. I would also like to thank Matt for making lab fun.

I would like to thank Mary-Kate Skoulos, Sara Supriyatno and Regina Zambrano. These three undergraduates volunteered ten to twenty hours a week to work on my thesis project. Having them gave was an enormous responsibility to guide them as scientists. I am so blessed to have such intelligent, capable and enthusiastic women give me their time and energy. In return they gave my project more structure, and sharing what I have learned with them made the research much more rewarding. I look forward to continue to be a part of their lives and can't wait to see what the future holds for them.

I would like to thank my classmates Ifeanyi Obiorah, Wahida Ali and Jason Hall. Both Ifeanyi and Wahida had every confidence that I would complete my doctoral studies and do so

well. I would like to thank Jason Hall for getting me through the first two years of graduate school classes. With an infant at home, Jason made sure I stayed awake in class and he also came to school on the weekends to study with me.

I would like to thank my husband, Atsushi Nakagawa, and my daughter Bianca Ai Nakagawa. When I asked Atsushi if he would mind if I went to graduate school for five years, he was fully supportive. I want to thank Bianca for being excited about coming with me to "frog school" and for reminding me that "science girls can do anything."

I would like to thank my parents for their confidence in my abilities and support for my studies, from pre-K to the 25th grade. My parents graciously allowed my family to live with them when we first moved to Long Island, and throughout my graduate studies have supported me by caring for my daughter, cooking food and lending an ear. I would also like to thank my Aunt Barbara Sabatino for babysitting and taking my family in for a time. I could not have done this without your sanity or support.

I would like to thank my Hakodate, Japan family, especially my host-parents Ryuji and Emiko Sato for their undying belief in my abilities and for adopting me as their "fifth daughter." During that short summer that I lived with them, and in the visits, phone calls and e-mails since, Ryuji and Emiko have taught me much about being a person of quality. I can't thank them enough for their love and support.

Lastly, figures republished Tuzer Kalkan et al., 2009, have been reprinted with the written permission of the the American Society for Cell Biology, which publishes the Molecular Biology of the Cell journal (license number 3687081149425).

Chapter 1: Introduction

1.1.1 Tumor Necrosis Factor Receptor-Associated Factors (TRAFs)

The TRAF family of adaptor proteins were discovered when TRAF1 and TRAF2 were identified as proteins required for Tumor Necrosis Factor-Receptor 2 (TNF-R2) cytosolic signaling. Tumor Necrosis Factor (TNF) is a cytokine released by activated macrophages that plays an important role in inflammation, cytotoxicity, immunoregulation, proliferation and anti-viral defense. Extracellular TNF cytokines are received by transmembrane TNF receptors, which transduce the signal intracellularly. TNF-R, like other members of the TNF receptor superfamily, do not contain a cytosolic tyrosine kinase domain (Rothe et al., 1994), therefore, signaling from the activated receptor must work through associated proteins. In order to find these proteins, a region of the intracellular TNF-R2 domain that is known to mediate TNF signaling was used in a yeast two hybrid screen for binding partners involved in transducing TNF signals.

TRAF1 and TRAF2 were found to bind the intracellular domain of the receptor and be involved in downstream signaling. They were named TNF receptor-associated factors (TRAF), due to their association with TNF receptors and their c-terminal domain that bound to the TNF receptors was named the TRAF domain. To date, there are six TRAF domain containing family members named TRAF1 through TRAF6. Additionally, TRAF7 was added to the family, though the designation as a TRAF is controversial due to its lack of a TRAF domain. A typical TRAF, (TRAFs 2-6), contain an N-terminal RING domain followed by five to seven zinc fingers, a coiled-coil and a C-terminal TRAF domain. TRAF1 lacks a RING domain, and contains one zinc finger and a TRAF domain, whereas TRAF7 Contains an N-terminal RING domain, followed by one zinc finger, a coiled coil and seven WD40 repeats. TRAF7 will not be discussed further in this dissertation, and the word TRAF will refer to TRAFs 1 through 6.

A functional TRAF protein is a trimer of three TRAF monomers, and formation of a trimer is dependent on the TRAF domain. A trimerized TRAF domain can be compared to the shape of a mushroom, with the coiled-coil N-TRAF domain as the stalk and the C-TRAF domain as the

cap. Trimerization is determined by the coiled-coil domain, where some allow for TRAF homo and heterotrimerization, while others form only homotrimers. The C-TRAF domain alone does not appear sufficient for TRAF protein trimerization as TRAF2 C-TRAF domains missing the coiled-coil region remain as monomers in solution (Park et al., 1999). The C-TRAF domain is composed of roughly 180 amino acids forming 7 to 8 anti-parallel β-sheets (Park et al., 1999). The C-TRAF domain is similar to a C-terminal domain found in meprin proteins, a family of extracellular metalloproteases, which also forms 7-8 anti-parallel β-sheets. Due to this homology, the C-TRAF domain is also referred to as the Meprin and TRAF homology (MATH) domain. The TRAF memprin and TRAF homology (MATH) domain or C-TRAF domain, has been found as distantly as protozoa, suggesting that the domain evolved very early in the evolution of eukaryotes (Zapata et al., 2007). The MATH TRAF domain is needed for many protein-protein interactions, and TRAFs loose their membrane binding affinity when the TRAF domain is removed (Glauner et al., 2002).

Often proteins that contain MATH domains also contain ubiquitin E3 ligase activity (Zapata et al., 2007). Indeed, TRAFs 2-6 contain a RING (Really Interesting New Gene) domain, which are E3 ubiquitin ligases. TRAF proteins are able to function as E3 ubiquitin ligases without being a part of a large protein complex, and TRAF2 and TRAF6 are able to catalyze K63-linked polyubiquitination, which mainly regulates protein function (Deng et al., 2000), and TRAF2 is able to modulate protein activity through K63 linked ubiquitin chains. TRAF42 participates in a ubiquitin ligase complex containing cIAP1/cIAP2/ TRAF2, which modulates IKKε activity by polyubiquitinating IKKε (Zhou et al., 2013). Additionally, TRAF6, together with the ubiquitin-conjugating enzyme complex Ubc13/Uev1A is able to activate IKK signaling through k-63 linked polyubiquitin chains (Deng et al., 2000).

Unlike the RING and TRAF domains, all TRAFs contain at least one zinc finger domain. TRAF1 and 7 contain one zinc finger, TRAFs 2,3,5 and 6 contain five and TRAF4 contains seven (Fig. 1.1) (Xie, 2013). The zinc fingers are needed for some protein binding interactions, but their role is not as well defined as the RING and TRAF domains. TRAF2 activation of NF-κB requires the RING domain and the zinc fingers, but here too, the exact role of the zinc finger domain is not defined (Takeuchi et al., 1996).

1.1.2 TRAF4: Tumor Necrosis Factor Receptor-Associated Factor 4

Interestingly, TRAF4 is unable to bind TNF receptors and is sometimes referred to as the unique member of the TRAF family. Closer examination of the TRAF domain of TRAF4 shows two unique features, first the coiled-coil domain is much shorter than other TRAF family members, and is thought to be the reason why TRAF4 has only been shown to form homotrimers (Rousseau et al., 2011). Secondly, the MATH domain of TRAF4 is missing three key amino acids that allow other TRAF family members to bind TNF-receptors, suggesting that TRAF4 functions separately from TNF signaling (Fig. 1.2) (Kedinger and Rio, 2007).

TRAF4 is highly conserved with the phylogeny of the TRAF family showing that TRAF6 evolved first, followed by TRAF4, with TRAFs 1,2,3 and 5 evolving later in mammals from a common precursor (Fig. 1.3)(Grech et al., 2000). TRAF4 is found in drosophila, zebra fish, Xenopus, and mammals, and has been shown to have ontogenic functions in many organisms. Drosophila TRAF4, (dTRAF1), is expressed within the developing nervous system and is found in epithelial progenitor cells, similar to the expression pattern seen in mammals. (Masson et al., 1998; Preiss et al., 2001).

1.1.3 Early Xenopus Embryonic Development

The early embryo develops three germ layers very early in development that are the origin of all organs and tissues of the developing animal. The germ layers are created during the process of gastrulation when presumptive mesoderm cells involute, pulling themselves inside the embryo and in between the ectoderm and endoderm. Once gastrulation is completed, the embryo has an alimentary canal that runs from mouth to anus. In Xenopus, gastrulation begins with the formation of a dorsal lip, a group of cells that involute and move inside the embryo. By stage 11, the blastopore lip encircles the vegetal side of the embryo and gradually constricts until it appears as a dot marking the anus. Closure of the blastopore marks stage 13 and the beginning of neurulation in Xenopus.

The TGF-β superfamily of signaling factors play an essential role in the induction and patterning of the early embryonic germ layers, morphogenetic movements of gastrulation and dorso-ventral patterning of the embryo. Within the TGF-β superfamily, two activating ligands,

Nodal and BMP, will be at the center of this study. Nodals are necessary for the induction of the mesoderm and for dorsal patterning, while BMPs are necessary for induction of the epidermis and ventral pattering. It is still unclear, however, how TGF-β signaling can give rise to different tissue types at different thresholds of activity. Therefore, studies into how proteins like TRAF4 regulate TGF-β signaling activity increases our understanding of how the embryo tightly controls cell fate decisions.

Induction of the early embryonic germ layers requires maternally placed and vegetally located transcripts of VegT. VegT is a T-box transcription factor that activates the transcription of TGF-β ligands (Hill, 2001). Activation of TGF-β signaling, as measured by activated Smad levels, are not found until after the midblastula transition, which marks the beginning of zygotic transcription and coincides with the induction of the mesoderm (Faure et al., 2000). VegT and Vg1 induce vegetally located Nodals, a TGF-β extracellular ligand that activates signaling. Inhibition of Nodal signaling results in the loss of mesoderm (Agius et al., 2000), suggesting that Nodals are necessary for mesoderm induction. Nodals are present in a gradient from dorsal to ventral (Agius et al., 2000), and are needed for dorsal structures. Another TGF-β activating ligand, BMP4 is also expressed in a gradient. As the dose of BMP4 increases, muscle, pronephros and blood are induced (Dosch et al., 1997), showing that BMP4 has the ability to induce tissues in a dose-dependent manner representative of a morphogen. Surprisingly, BMP, as well as Nodal signaling, is required for mesoderm formation as mice with homozygous mutations for BMPR-II receptors were unable to produce mesoderm (Beppu et al., 2000).

Neural differentiation of the ectoderm, in contrast, requires the suppression of BMP signaling at many levels (Kuroda et al., 2005; Sasai et al., 1995). Extracellular inhibitors of BMP ligands, such as Chordin and noggin, are expressed by the Spemann organizer and prevent BMP signaling in the neural-ectoderm (Piccolo et al., 1996; Zimmerman et al., 1996). Additionally, intracellular inhibitors of receptor complex formation, receptors and Smads, also work to inhibit BMP signaling (Shi and Massagué, 2003), whose regulation is important for the fate of the ectoderm.

The ectoderm, one of the three germ layers that make up the early embryo, is the origin of the epidermis and central nervous system. In the mid 1990's it became clear that BMPs could induce epidermis (Wilson and Hemmati-Brivanlou, 1995). Eventually, isolated ectoderm, when left intact during gastrulation, was shown to become epidermis, and when

dissociated and reaggregated after gastrulation, became neural structures (Grunz and Tacke, 1989; Sato and Sargent, 1989). These experiments were the first to bring up the possibility that there may not be an extracellular inducer of neural tissue. Later, inhibitors of BMP ligands found in the Spemann organizer were shown to induce neural induction (Lamb et al., 1993). And BMP expression was shown to peak in caps during gastrulation. Together, these experiments strongly supported BMP inhibition as necessary for neural induction instead of a specific neural morphogen.

The role of BMP signaling and its inhibitors was further defined within the fate of the epidermis by testing if BMP inhibitors, when removed, would reduce neural induction of the epidermis. When the BMP inhibitors follistatin, chordin and noggin are all knocked down with the injection of translation blocking morpholinos, the epidermis expands into the region of the neural ectoderm (Khokha et al., 2005). This experiment, in addition to the dissociation experiments and others, showed that the differentiation of the isolated ectoderm into either epidermis or neural tissue corresponds to the level of BMP signaling activity.

In a normally developing whole embryo, BMP signaling is essential for patterning ventral structures, including the epidermis and belly tissues. Ventrally localized BMP signals are needed for epidermal differentiation in the ectoderm and ventral patterning of the mesoderm. Overexpression of BMP4 in the early embryo can expand ventral tissues, and at high enough doses, ventralize dorsal tissues (Hemmati-Brivanlou and Thomsen, 1995). At high enough doses, exogenous BMP4 prevents formation of the blastopore, (a dorsal structure), and results in embryos that fail to gastrulate. Therefore a rescue of the ability to gastrulate in embryos overexpressing BMP may suggest a reduction in BMP signaling activity.

Early neural differentiation in the Xenopus ectoderm requires BMP4 suppression in addition to Sox2 expression. Sox2 is expressed dorsally throughout the ectoderm of the gastrula (stage 10-12), and within the neural-ectoderm of neurula through tail bud stage embryos (stage 13-24) (Cao et al., 2012; Wills et al., 2010). Without functional Sox2, inhibition of BMP signaling is not sufficient for neural induction of the ectoderm (Kishi et al., 2000). Therefore, Sox2 can be used as a marker of early neural differentiation as it is not expressed in the epidermal ectoderm (Wills et al., 2010). Here I test if TRAF4 is necessary for robust BMP signaling and the differentiation of the epidermis by asking if

knockdown of TRAF4 in animal caps can induce neural differentiation marked by expression of neural markers such as Sox2.

1.1.4 Intracellular TGF-β signaling

TGF-β signaling can be visualized as beginning in the extracellular space with the release of immature pro-ligands. The pro-domain of the ligand must be cleaved to create a functional ligand that can dimerize and activate its receptors. If cleavage does not occur properly, the ligand is degraded by the lysosome (Goldman et al., 2006). Mature ligands form a dimer, and each combination of hetero or homodimer have different receptor affinities that result in ligand-dimer specific receptor binding. A functional ligand-dimer binds to the extracellular region of a TGF-β transmembrane receptor complex. TGF-β receptors are a tetramer of two type I and two type II subunits (Kingsley, 1994). Binding of the ligand-dimers to a homodimer of receptor subunits is necessary for the receptor complex to form, as the extracellular domains of the receptors do not touch each other and seem to be held together in some part by ligand binding (Allendorph et al., 2006).

Formation of a receptor complex allows the constitutively active intracellular kinase domain of the type II receptor to phosphorylate and activate the cytosolic serine/threonine kinase domain of the type I receptors (Wrana et al., 1994). There are seven type I receptors and five type II receptors identified so far, and can be paired into different combinations that lead to different downstream consequences (Kishigami and Mishina, 2005).

Signals move from TGF-β transmembrane receptors to the nucleus through transcription factors called Smads. Activated type I receptors recruit and phosphorylate receptor activated Smads (R-Smads) by phosphorylating their c-terminus. There are five R-Smads, which are activated specifically in response to an active ligand/receptor complex. The BMP branch of TGF-β signaling works through Smad1, Smad5 and Smad8, and the Nodal branch works through Smad2 and Smad3 (Kishigami and Mishina, 2005). R-Smads can form hetero or homo dimers with Smads that act within their branch of the signaling pathway. Activated R-Smads from both branches create a trimer with a co-Smad (Smad4), and competition for Smad4 can regulate signaling activity (Labbé et al., 1998). Once formed, the Smad trimer can enter the nucleus and

form a transcription complex that regulates gene transcription specific to the combination of ligand/receptor used to activate signaling.

1.1.5 Inhibition of TGF-β Signaling

TGF-β can be regulated at many points along the signaling cascade. Extracellular inhibitors can bind TGF-β ligands and prevent them from binding receptors (Balemans and Van Hul, 2002). Intracellularly at the membrane, Smad7 prevents the activation of Smad1 and Smad2, and Smad6 can inhibit Smad transcriptional activity by competing with Smad1/5 for Smad4 (Hata et al., 1998). Also, the duration of R-Smad activity can be modified through phosphorylation of the central linker region that connects their two functional domains. Phosphorylation at the linker by CDK8 and CDK9 promotes Smad transcriptional activity and subsequent degradation by the proteasome (Alarcón et al., 2009). Within the nucleus, the Smad transcription complex can be inhibited by a number of repressor complexes including ski (Wang et al., 2000).

In the cytosol, Smads can be inhibited by Smurfs (Smad ubiquitination regulatory factor); ubiquitin ligases that target Smads for degradation by the proteasome. Smurf1 negatively regulates BMP signaling through ubiquitylation of Smad1 and Smad5, targeting them for proteasomal degradation (Alexandrova and Thomsen, 2006). When Smurf1 was knocked down dorsally, embryos presented defective neural folding and microcephaly (Alexandrova and Thomsen, 2006), suggesting that inhibition of BMP signaling intracellularly is necessary even when extracellular inhibitors are abundant.

1.1.6 TRAF4 is a target of Smurf1

In order to possible targets of Smurf1 ubiquitination and possible effectors of TGF-β signaling, the Thomsen lab performed a yeast two-hybrid screen using Smurf1 as bait. This screen found TRAF4 to bind Smurf1, while later studies gave evidence that Smurf1 targets TRAF4 for degradation by the proteasome (Kalkan et al., 2009). Smurf1 that is unable to ubiquitinate substrates, but not wild type Smurf1, is able to pull down TRAF4. In addition, when the proteasome was inhibited with MG132, wild type Smurf1 was also able to pull down TRAF4, suggesting that TRAF4 is degraded by the proteasome when wild-type Smurf1 is

present. When TRAF4, Smurf1 and ubiquitin are overexpressed together, Immunoprecipitation of TRAF4 gives a smear of varying sizes on a western blot suggesting there are chains of ubiquitin of varying lengths. Additionally, Smurf1 and TRAF4 colocalize in HeLa cells, and when Smurf1 is knocked down in these cells, TRAF4 levels increase. Together, these experiments point to TRAF4 being ubiquitinated by Smurf1, targeting TRAF4 for degradation by the proteasome.

1.1.7 TRAF4 within TGF-β signaling

After seeing that Smurf1, (an inhibitor of TGF- β signaling), negatively regulates TRAF4, and that TRAF4 is expressed within the ectoderm and mesoderm(Kalkan et al., 2009), tissues where TGF-β signaling is necessary for healthy development, TRAF4 was examined further for functions within TGF-β signaling. To do so, the isolated Xenopus animal cap was used as a model system for mesoderm induction. The animal cap is fated to become ectoderm, however, overexpression of BMP4 can induce the cap to become ventral mesoderm. Kalkan et al. tested if overexpression of TRAF4 altered BMP signaling in isolated animal caps. TRAF4 was co-injected with a dose of BMP4 that only minimally activated BMP signaling. Co-injection resulted in a large increase in downstream markers of BMP signaling over injection of BMP4 alone (Fig. 1.5A). Surprisingly, injection of TRAF4 alone did not increase these markers above background levels, suggesting that some level of BMP signaling is necessary for TRAF4 to potentiate downstream BMP markers.

Next, Kalkan et al. asked if TRAF4 can potentiate BMP signaling by testing if overexpression of TRAF4 can reduce neural induction after BMP signaling is inhibited. A BMP receptor missing the cytosolic kinase domain needed for Smad activation resulted in animal caps with sharp increases in the neural and anterior markers NCAM and XAG-1 (Fig. 1.5B). This experiment again shows that isolated animal caps, when untreated, develop into epidermal tissues, but when BMP signaling is blocked, the animal cap will develop into neural tissues. When TRAF4 was co-injected with the truncated BMP receptor, NCAM and XAG-1 levels dropped significantly, suggesting that BMP signaling is increasing. Together, these experiments suggest that TRAF4 positively regulates BMP signaling.

Kalkan et al. also asked if TRAF4 could positively regulate the Nodal side of TGF-β signaling. When TRAF4 was co-expressed with Xenopus Nodal-related 2 (Xnr2) the addition

of TRAF4 resulted in greater levels of downstream markers of Xnr2 signaling than when Xnr2 was injected alone. In this case as well, overexpression of TRAF4 alone was not sufficient to induce markers of Xnr2 signaling. Next, they asked if loss of TRAF4 could inhibit the induction of markers of Xnr2 signaling. To do so, Xnr2 was co-injected with a TRAF4 morpholino oligonucleotide that specifically blocked translation of TRAF4A. Co-injection of Xnr2 and the TRAF4A morpholino reduced Xnr2 marker expression when compared to injection of Xnr2 alone (Fig. 1.6B). Here as well, TRAF4 is seen to positively regulate TGF-β branch of Nodal signaling.

Additionally, TGF-β signaling induces K63 polyubiquitination of TRAF4, peaking 30 minutes after TGF-β stimulation (Zhang et al., 2013). Polyubiquitination is not seen when the RING domain of TRAF4 is removed. This may suggest that TGF-β activation is activating TRAF4 through a yet to be determined mechanism. Together these data suggest that TRAF4 is a positive regulator of both the Nodal and BMP branches of TGF-β signaling. However, how TRAF4 functions in cell fate decisions is still not well understood.

With the knowledge that TRAF4 has the ability to potentiate both the Nodal and BMP side of TGF-β signaling, I asked if TRAF4 is participating in the differentiation of the ectoderm

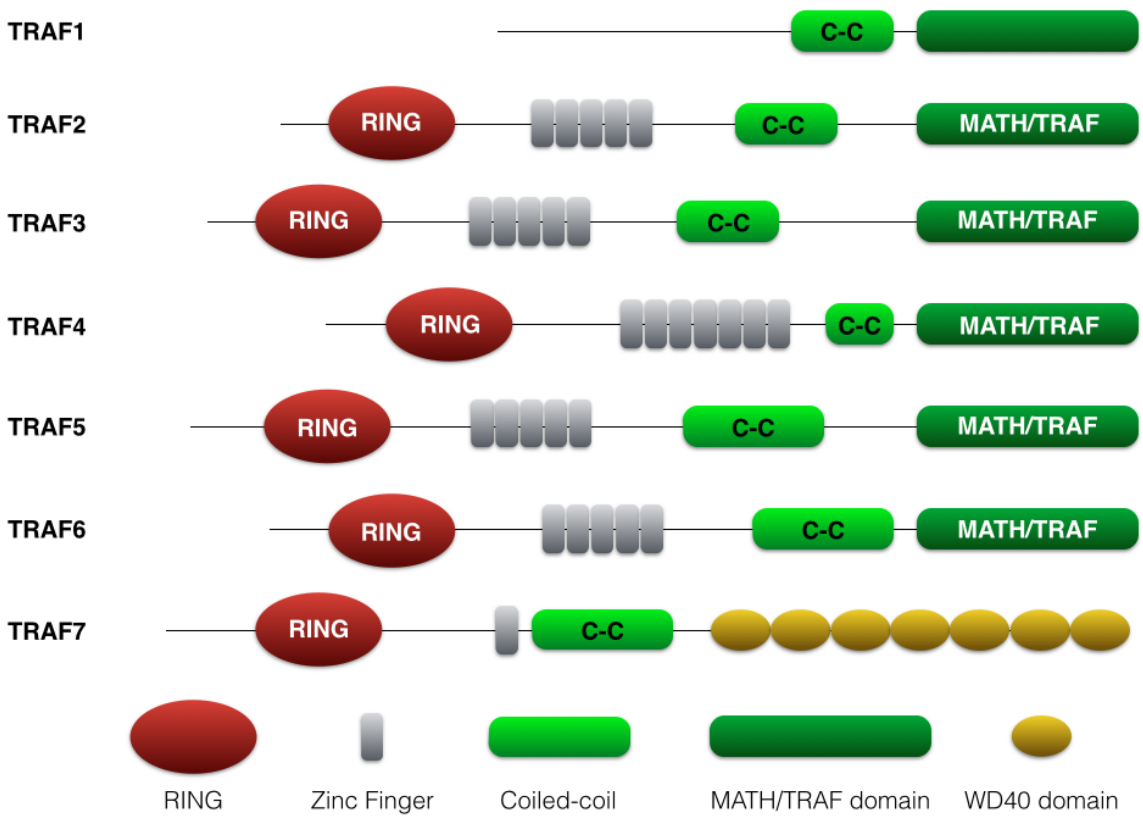

Figure 1.1 | Protein domains of the TRAF family of proteins. To date, seven proteins have been designated as TRAFs and are numbered by their order of discovery. A typical TRAF protein contains a RING (Really Interesting New Gene) domain, zinc fingers, a coiled-coil and TRAF domain. TRAF proteins are named for their c-terminal TRAF domain making TRAF7 a controversial member of the family as it does not contain a MATH/TRAF domain. *(Figure adapted from Zotti et al., 2011.)*

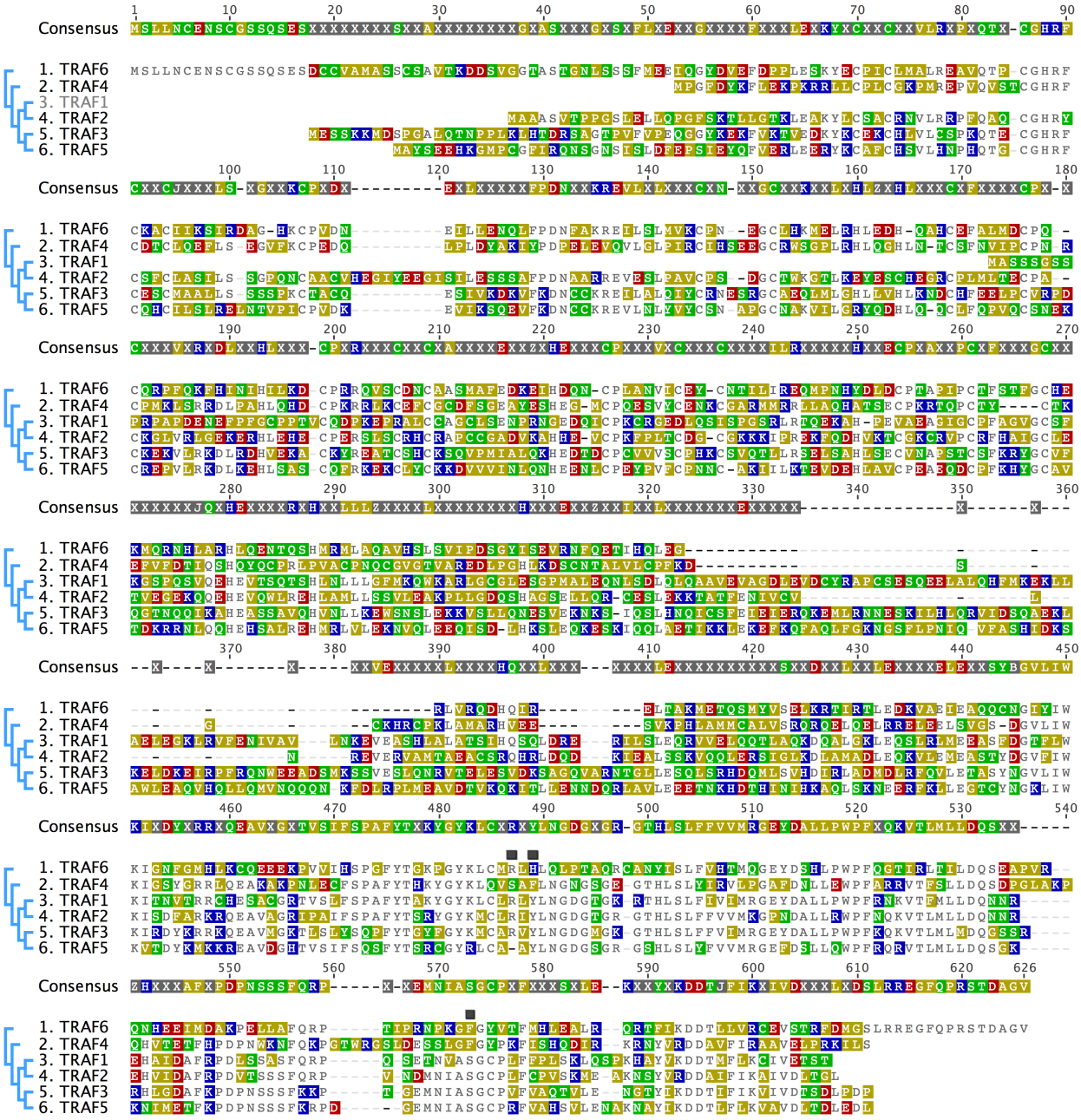

Figure 1.2 | Alignment of the TRAF domains of TRAFs 1-6. The TRAF domains of homo sapiens TRAFs 1-6 are listed in evolutionary order according to the blue brackets. Residues are colored by polarity: yellow – non-polar; green – polar, uncharged; red – polar, acidic; blue – polar, basic. Three gray squares denote the three amino acid residues needed for TNF receptor binding (*residues 487, 489 and 573*)(Kedinger and Rio, 2007).

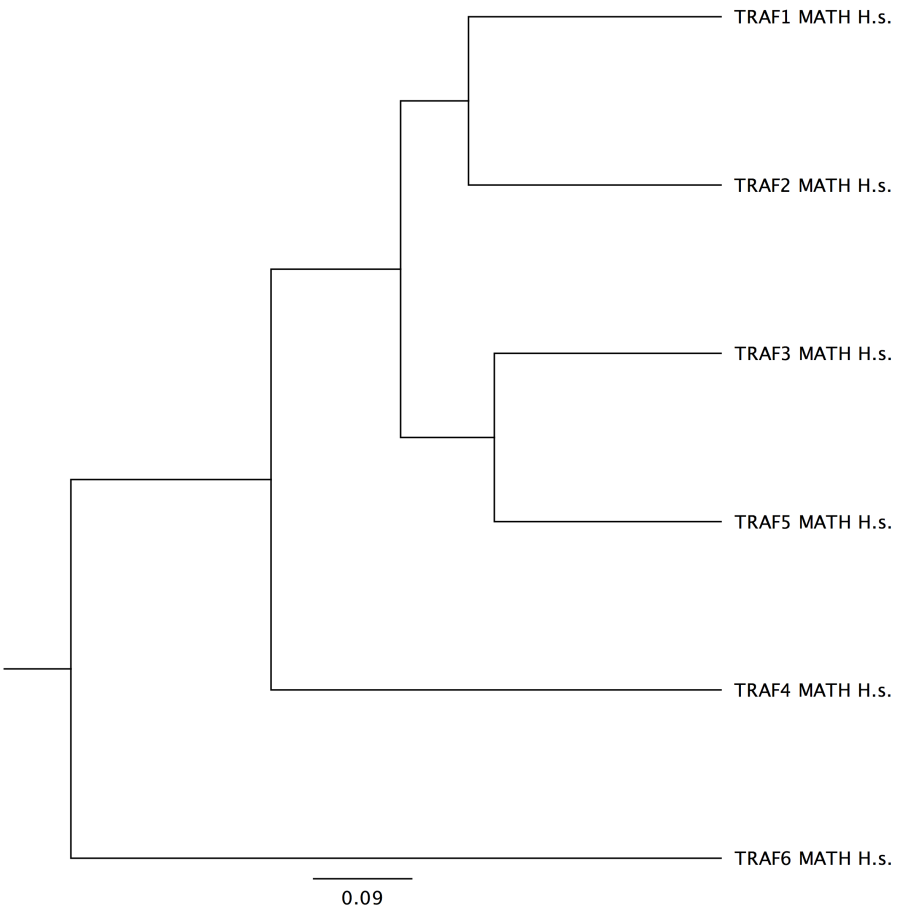

Figure 1.3| Phylogenic tree of the TRAF domain of TRAFs 1-6. TRAF6 evolved first followed by TRAF4. Later, TRAFs1,2,3 and 5 evolved. The tree was created in Geneious version 8.1.

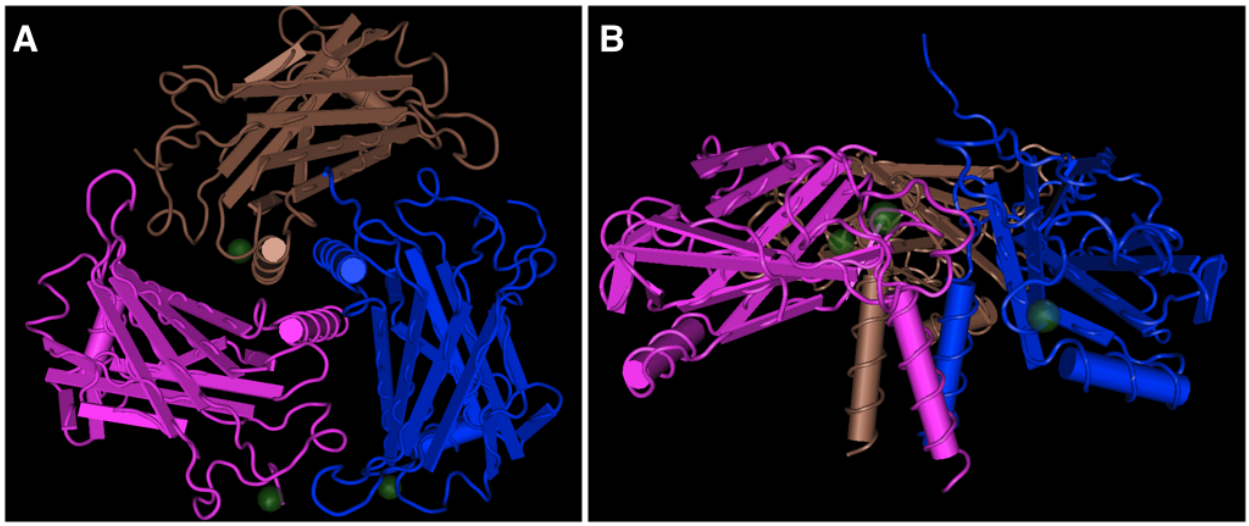

Figure 1.4 | Crystal structure of the H.s. TRAF4 TRAF domain. A ribbon diagram of three TRAF domains forming one trimer of TRAF4 at 1.8 Å. (**A**) Top down view of the MATH/TRAF domain. (**B**) Side view of the TRAF domain showing the MATH/TRAF domain mushroom-like cap and coiled-coil domain stalk. (Rousseau et al., 2013)(*MMDB ID: 115595PDB; PDB ID: 3ZJB*).

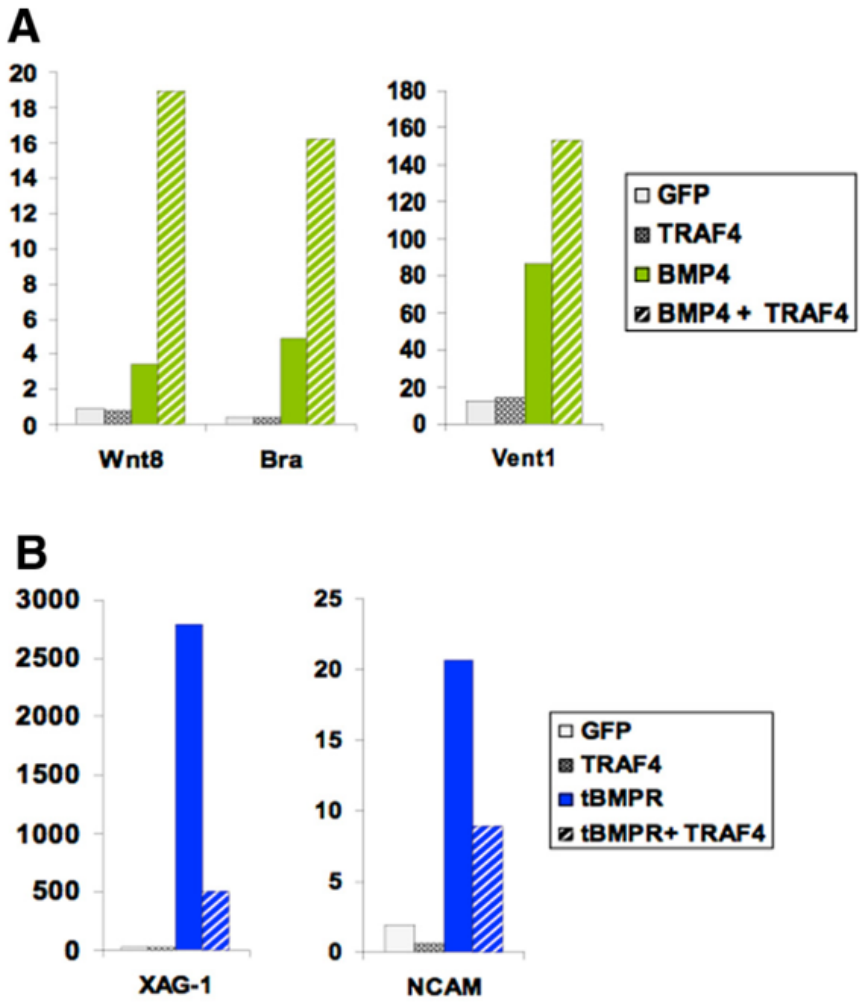

Figure 1.5| Overexpression of TRAF4 potentiates BMP signaling. BMP4 or a dominant-negative truncated BMP receptor was overexpressed with and without TRAF4A RNA in stage 10.5 isolated *Xenopus laevis* animal caps. (**A**) BMP4 overexpression resulted in minimal induction of mesoderm markers Wnt8, Bra and Vent1. Co-injection with TRAF4 greatly increases marker expression. (**B**) Co-injection of a truncated BMP receptor and TRAF4A RNA greatly reduce induction of neural and anterior markers NCAM and XAG-1. Figures are taken from Kalkan et al., 2009.

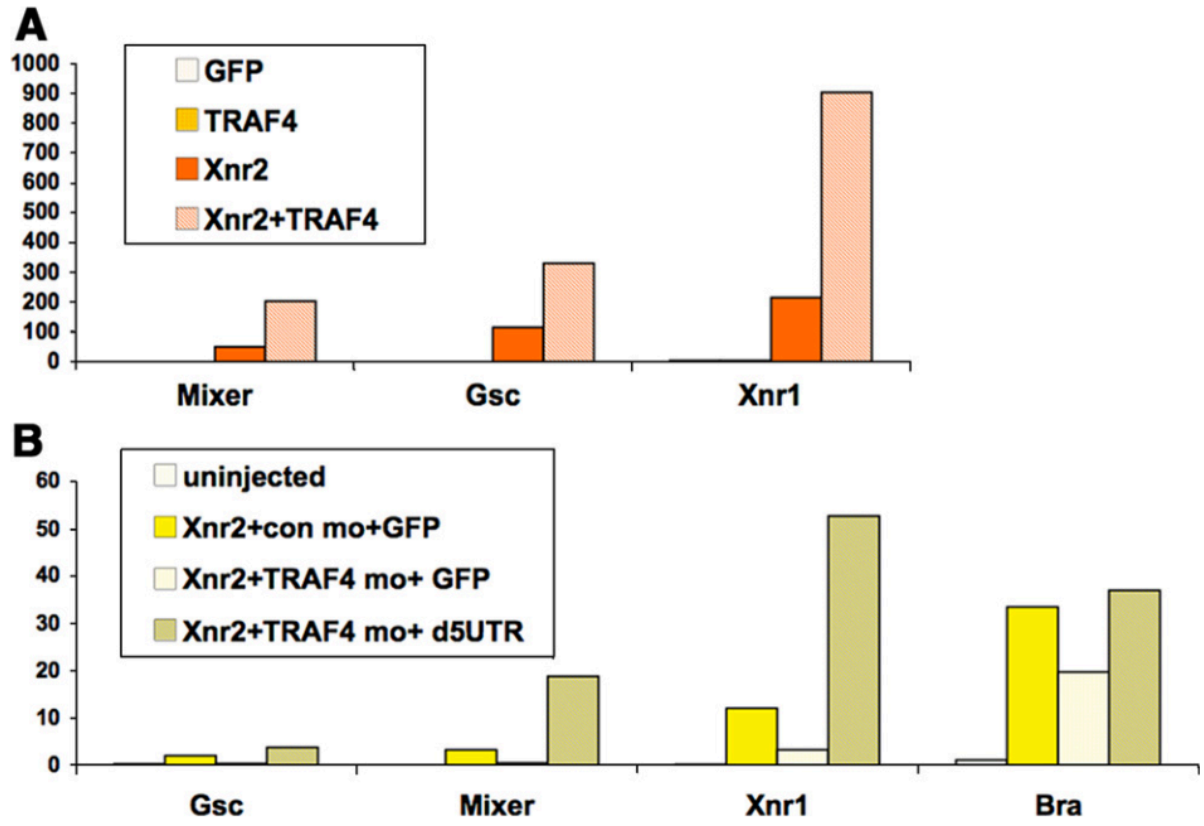

Figure 1.6 | TRAF4 potentiates signaling through Nodal. (**A**) Co-injection of Xnr2 with TRAF4A RNA greatly increases induction of mesoderm markers over Xnr2 alone. (**B**) Co-injection of Xnr2 with a TRAF4A MO reduces mesoderm marker expression when compared to injection of Xnr2 alone. Marker expression is rescued when MO resistant TRAF4A RNA is also injected. Figures are taken from Kalkan et al., 2009.

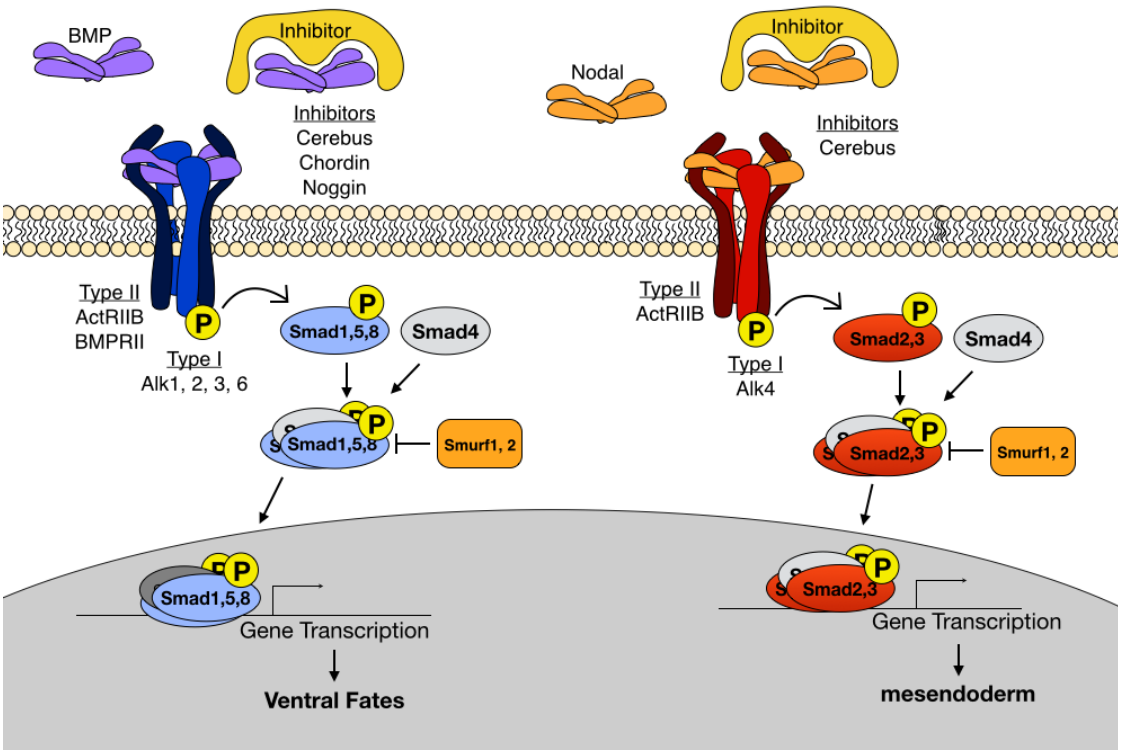

Figure 1.7 | TGF-β signaling. Extracellular ligands BMP and Nodal binding results in a receptor tetramer of two type one and two type II transmembrane receptors. The constitutively active type II receptors phosphorylate and activate type I receptors, which can then phosphorylate and activate intracellular signaling molecules called Smads. Activated Smads form a trimer with Smad4 and enter the nucleus where they direct gene transcription in accordance to the ligand receptor complex that was activated (Feng and Derynck, 2005). Signaling can be inhibited extracellularly through inhibitors of the ligand or intracellular through Smurfs.

CHAPTER 2: TRAF4 is necessary for anterior development

2.1 INTRODUCTION

2.1.1 Xenopus laevis: a model organism for embryonic development

Xenopus laevis, the African clawed frog, was brought to Europe in the first half of the 19th century, however, it was not commonly seen in North American laboratories until its use as a pregnancy test in the late 1930's (Gurdon and Hopwood, 2000). In 1930, Lancelot Hogben reported that after hypophysectomy, (removal of the pituitary gland), the ovaries involuted, while injection of anterior pituitary extracts induced ovulation. *Xenopus laevis* was soon shown to respond to the urine of pregnant women, when within 24 hours of injection with a positive sample, the frog laid eggs. By 1939, *Xenopus laevis* was the preferred pregnancy test due to its ease of use over mouse or rabbit (Gurdon and Hopwood, 2000).

During this time *Xenopus laevis* husbandry became well defined, and due to the ease of inducing ovulation, *Xenopus laevis* soon became popular as a model of embryonic development. *Xenopus laevis* can lay hundreds of eggs at a time, and when fertilized with fresh testes, can produce fertilization rates close to 100%. The rate of development can be sped up or slowed down according to the incubation temperature and the researchers needs, and these embryos can develop on the bench top in pond water, making them easy to care for.

Xenopus laevis embryos are also tolerant of manipulation, as each cell of the early embryo contains yolk proteins, allowing these cells to grow independently of the whole embryo until an equivalent uncut sibling embryo develops into an early tadpole and needs to feed. This allows for experiments where whole sections of the embryo are isolated and grown independently, or transplanted to other embryos. The ability to manipulate these embryos allows scientists to research the specific fate of a tissue, and ask questions into cell autonomy. Additionally, the fate map of *Xenopus laevis* is very consistent and is mostly established by the first cleavage. This gives a strong degree of certainty as to which

section of the embryo will develop into which tissues in the fully formed tadpole, allowing for injection and manipulation of specific tissues (Moody, 1987).

2.1.2 TRAF4 is present as two homeologs in Xenopus laevis

The African clawed frog *Xenopus laevis* is the product of an interspecific hybridization that produced a whole genome duplication event 21-40 million years ago, creating an allotetraploid species (Uno et al., 2013). In *Xenopus laevis*, most genes are present as two homeologs and are cataloged as an A and B form. Indeed, TRAF4 is also present as two homeologs in *X. laevis* dubbed TRAF4A and TRAF4B for the order they were discovered. Homeologs have the potential to diverge more quickly than the genes of a diploid species as there is a second copy to maintain the original function. Therefore homeologs may present large differences in expression levels and expression patterns (Hellsten et al., 2007). Investigations into the contributions or functions of the two homeologs can be accomplished by creating probes and tools from mRNA sequences that differ between the two homeologs. Expression patterns can be visualized through in situ hybridization by creating probes specific to less identical sections of the UTRs. Additionally, homeolog expression levels can be individually tested through Real Time PCR by making primers against distinct regions of the UTRs (Kalkan et al., 2009).

The homeologs can also be specifically knocked down in *Xenopus laevis* embryos by blocking their translation. This can be accomplished with short oligonucleotide sequences that bind complimentary to the mRNA transcript of a gene-of-interest within roughly 80 bases upstream of the translational start codon (Eisen and Smith, 2008). These translation-blocking oligomers are called morpholinos (MO) for the morpholine ring that makes up their backbone and prevents them from degradation by endonucleases (Eisen and Smith, 2008). Binding of the MO to its target sequence creates a double stranded section of mRNA that prevents the ribosome from reading the transcript, thus preventing translation. MOs specific to one transcript are usually possible with sequences longer than 18 bases, as a sequence of 18 bases or more is unlikely to be found in more than one transcript, often leading to MO specificity (Summerton and Weller, 1997).

In addition to the use of morpholino oligonucleotides to inhibit translation and knockdown protein levels, overexpression of a gene-of-interest can also be used to gain insight into the function of a protein. Synthetic RNA transcripts can be injected into a specific region of interest. For example, the presumptive epidermis or neural tissues can be targeted through injection into the animal cap. However, if the injections are made at the two-cell stage, some of this RNA can diffuse into the endoderm and other unintended areas. Therefore, overexpression results in the translation of the mRNA in areas of the embryo where the endogenous mRNA may not be normally expressed.

2.2 Results

2.2.1 TRAF4A is likely more similar to an evolutionary precursor of Xenopus laevis TRAF4.

Xenopus laevis has two homeologs of TRAF4 named TRAF4A and TRAF4B, however, it is not clear if, or by how much the homeologs have diverged in function or in expression. Comparing the nucleotide sequences of the homeologs to the sequence of TRAF4 in a diploid Xenopus species can give clues as to which homeolog has remained less changed, and perhaps give evidence for one homeolog being more functionally similar to the single TRAF4 found in diploid species. Here, the 5' untranslated region (UTR) of *Xenopus tropicalis* and the 5' UTRs of the two *Xenopus laevis*

homeologs were aligned in order to see if one *X. laevis* homeolog is more similar to *X. tropicalis*. To do so, the same length of bases, in this case 128 bases upstream and 12 bases downstream of the AUG translational start site, were used for comparison (Fig. 2.1). Alignments were created on Geneious version 8.1, which also gave the percent identity of the aligned sequences.

The alignment shows the 5' UTR of TRAF4A to be more similar to *X. tropicalis* than TRAF4B, sharing 73% identity with *tropicalis* and 36% identity with TRAF4B. When the coding sequences were compared (Fig. 2.2), *X. laevis* TRAF4A is nearly as similar to *X. tropicalis* as it is to TRAF4B, (93.489% and 93.984% respectively). TRAF4B shares 91.932% identity with *X. tropicalis*, slightly less than the shared identity between TRAF4A and *X. tropicalis*. Here in the coding region too, TRAF4A shares more similarity to *X. tropicalis* than TRAF4B.

The 3' UTRs were also aligned and compared for shared identity. The alignment uses the last nine bases of the coding sequence and the stop codon, and the first 900 bases of the 3' untranslated regions. The published 3' UTR sequence of TRAF4A (see figure 2.1A) is 941 bases and is the shortest of the three, therefore, a 3' UTR length of less than 941 bases was chosen in order to compare sequences of equal lengths. Using equal lengths avoids lowering the percent identity due to missing sequence, and not necessarily due to a lack of identity, as is the case when the full length published 3' UTR sequences of TRAF4A and TRAF4B are aligned, they share 59.88% identity (data not shown). However, when an equal length of known

sequence of TRAF4A and TRAF4B 3' UTR is used for comparison, the identity is 80.3% (Fig. 2.3). When these three sequences were aligned, the 3' UTR of *X. tropicalis* shares 78.075% identity with TRAF4A and 77.614% identity with TRAF4B. TRAF4A and TRAF4B share 80.3% sequence identity. Here too, *X. tropicalis* is slightly more similar to TRAF4A, however, this difference is less than 1%.

2.2.2 Early expression of TRAF4B is within the ectoderm and neural structures.

The expression pattern of a gene gives clues as to which tissues the protein product may be functioning. To test if TRAF4B may also be playing a role in the developing ectoderm, the expression pattern of TRAF4B was examined using a TRAF4B specific probe complementary to a region of the TRAF4B 3' UTR. Using the full length NCBI published TRAF4B sequence (Fig. 2.1A), the probe begins at base 2,138 and ends at base 4,328, giving a total sequence length of 2,191 bases, and extending 2,720 bases past the published TRAF4A sequence. In situ probes were created as stated in section 5.6.

In situ staining of TRAF4B was performed in untreated embryos that were fixed prior to gastrulation (stage 8), during gastrulation (stage 11.5), at mid-neurula (stage 17) and early tail bud (stage 23) stages. TRAF4B staining is visible from the blastula through early tail bud stages (Fig. 2.5). In the stage 8 blastula, TRAF4B is present in the animal pole, and is limited to the presumptive ectoderm (A). Staining remains in the ectoderm in stage 11 gastrulae (B), and by stage 17, mid-neurula stage, TRAF4B staining is confined to neural tissues. In these embryos, staining can be seen in the neural plate (np) and neural folds. The dotted line in panel D defines the outline of the neural plate. By the early tail bud stage, stage 22, TRAF4B staining continues to be seen in anterior and neural tissues, including the cement gland (cg), eye (e), and ear vesicle (ev)(Fig. 2.5E). Staining is also seen in the midbrain and hindbrain, and continues along the spinal cord (sc) and somites (som)(Fig. 2.5F). This data visualizes TRAF4B expression from the early embryo until the early tail bud stages showing that TRAF4B is present in the early ectoderm and later in neural tissues.

2.2.3 TRAF4A and TRAF4B are expressed within the ectoderm.

In order to investigate if TRAF4 plays a role in the differentiation of the epidermis, a tissue derived from the ectoderm, I tested if TRAF4A and TRAF4B homeologs were expressed within the developing epidermis by using the *Xenopus laevis* animal cap assay. TRAF4 homeolog expression within the ectoderm was measured using RT-PCR. The raw data was processed using LinReg PCR and normalized to EEF1α. The graphed data of TRAF4A and TRAF4B (fig 2.7) are given as arbitrary fluorescent units (Ruijter et al., 2009a).

Untreated embryos were incubated at room temperature until stage 7, when the animal caps were removed and incubated in 0.5x MMR. Once sibling whole embryos reached the desired stages, the caps were frozen in 0.5X MMR at -80˚C. Caps were isolated and processed for RT-PCR as described in the methods. The data was normalized to eEF1α, and the initial cDNA concentrations were given a value in arbitrary fluorescence units (Ruijter et al., 2009a). This experiment was performed in triplicate with each data point being a mixture of 12 to 18 sibling animal caps, and each graphed data point being the average of four groups of siblings.

TRAF4 expression was examined from just before the mid-blastula transition (stage 7) through closure of the neural folds and development of the neural tube (stage 20). TRAF4 is present throughout early development, gastrulation and neural stages. At each stage tested, TRAF4A transcripts outnumber TRAF4B transcripts. At Stage 7, TRAF4A transcripts are 47-fold higher than TRAF4B. During gastrulation, TRAF4A expression drops to roughly 5-fold higher than TRAF4B. During neural development, stages 14, 17 and 20, Both TRAF4A and TRAF4B levels drop to less than one tenth of maternal TRAF4A levels. These data show that TRAF4A and TRAF4B are present in the ectoderm where TRAF4B is able to participate in differentiation of the ectoderm.

2.2.4 Loss of TRAF4 results in delayed gastrulation and developmental defects.

In order to examine how TRAF4 knockdown affects the developing embryo, and to gain insight into the contribution of each homeolog to early development, I examined the effects of knocking down each homeolog individually. I first tested if one TRAF4 homeolog MO or a mixture of TRAF4 homeolog MOs would be most effective at creating a knockdown phenotype (Fig. 2.6). TRAF4A, TRAF4B or a combination of the two morpholinos were injected into the

marginal zone of each blastomere of the two-cell stage embryo, for a whole embryo dose of 25 ng or 50 ng. Embryos were then incubated in 0.1X MMR and imaged at stage 28.

By stage 28, the blastopore of many embryos remained open, and instead of presenting ventrally, near the normal location of the anus, the open blastopore presents dorsally. Anterior and posterior structures were bent backward towards the dorsally located open blastopore. In these embryos, anterior structures develop to some extent. In a few cases cement glands are visible, and there appears to be some eye development. Convergence and extension movements in the trunk were impeded, and in most cases, posterior structures are unrecognizable. In cases where anterior structures were difficult to determine, anterior gave a more narrow and rounded appearance, whereas posterior was wider and contained a small central cleft (Fig. 2.6J,K,L).

Open blastopores were seen after injection of either TRAF4 homeolog morpholino, but the phenotype occurred at different doses. At 25 ng, the TRAF4A MO did not give a visible phenotype. However, when the TRAF4A MO was injected at 50 ng, embryos did not close their blastopores. The TRAF4B MO at 25 ng, however, produced results visibly similar to embryos injected with 50 ng of TRAF4A. At 50 ng of TRAF4B MO, the embryos had open blastopores and some lacked a recognizable anterior-posterior axis. Thus, the TRAF4B MO gave a more severe phenotype than the TRAF4A MO at an equivalent dose, making the TRAF4B MO a more potent tool.

2.2.5 The TRAF4B MO gives a more severe developmental phenotype.

After seeing that the TRAF4B MO gave a more severe phenotype at an equivalent dose of the TRAF4A MO, I asked if combining the morpholinos would give a more complete knockdown than either of the morpholinos alone. To do so, I compared the phenotype resulting from knockdown using the TRAF4A MO, the TRAF4B MO or a 1:1 ratio combination of the two. Morpholinos were injected into the marginal zone of each blastomere of the two-cell stage embryo, and embryos were incubated in 0.1X MMR until blastopore closure is complete at stage 13 (NIEUWKOOP and FABER, 1956) and then imaged.

These gastrula stage embryos were divided into three phenotypes: closed blastopore (a), deformed blastopore (b) and open blastopore (c). The closed blastopore appears normal as a small dot where the blastopore ring is no longer visible. Deformed blastopores do not appear as

a dot, many appear as a cleft, but there is no visible endoderm. Open blastopores are easily distinguished by the light color of the endoderm visible within the open blastopore. At stage 13, embryos injected with the TRAF4B MO alone displayed more open blastopores than a mixture of the TRAF4A and B MO or the TRAF4A MO alone (fig 2.5A).

Classification and quantification of phenotypes was repeated at the tail bud stage. The embryos could be classified into five groups: normal (a), mild (b), deformed (c), open blastopore (d), spherical (e), (fig 2.5C). Spherical embryos appear to have not gastrulated and remain spherical similar to a blastula embryo. Again at stage 32, the TRAF4B MO injected group shows the most severe phenotype, with most embryos being classified as spherical or with open blastopores showing a visible endoderm. These data also suggest that injection of the TRAF4B morpholino alone gives the more severe phenotype.

2.2.6 The TRAF4B MO alone gives a more severe phenotype than combinations of the TRAF4A and B MO together.

In order to confirm that indeed the TRAF4B morpholino alone gave the most severe phenotype, the TRAF4A and TRAF4B morpholinos were injected in at ratios of 1:1, 2:1 or 1:2 of TRAF4A MO:TRAF4B MO at a 30 ng or 50 ng whole embryo dose. In figure 2.9, in panels A and B, the left-most embryo is a normally developing control is pictured for comparison. In panel (A), embryos injected with a 1:1 ratio of TRAFA MO:TRAF4B MO at 30 ng, show a mild phenotype of a shortened torso and less defined anterior structures. At 50 ng, convergence and extension movements are disrupted producing even shorter embryos with their anterior and posterior ends bent dorsally, and tail structures that are not well defined. When the TRAF4A MO and TRAF4B MO are injected in a 2:1 ratio, these embryos give a phenotype that appears as the average of the 1:1 dose at 30 ng and 50 ng. Some embryos are bent due to incomplete convergence and extension movements, and some are mildly deformed with definable anterior structures and a slightly shorter A-P axis. At 50 ng of 2:1 TRAF4A:TRAF4B, embryos look very similar to the 1:1 A:B embryos. All embryos have shortened A-P axes and most are bent dorsally. Most lack anterior and posterior structures, displaying ill-defined tail structures and no eyes.

In figure 2.9B, a 1:2 ratio of TRAF4A MO:TRAF4B MO gave more severe phenotypes, with many embryos giving a nearly complete loss of anterior structures. For comparison, the

TRAF4B MO was injected alone at 33 ng and 20 ng doses in order compare the contribution of the TRAF4B MO alone to the TRAF4A:TRAF4B MO combinations at 50 ng and 30 ng. Here it appears that the TRAF4A MO is adding to the phenotype, as TRAF4B injected alone at 33 ng gave embryos with cement glands and more readily recognizable A-P axis than the 50 ng dose at a ratio of 1:2, TRAF4A:TRAF4B MO. In addition, the 50 ng 1:2 ratio of TRAF4A:TRAF4B group did not have a readily discernable A-P axis and many had open blastopores. Therefore, the TRAF4B MO appears to be responsible for most of the knockdown phenotype, but the TRAF4A MO does contribute to some degree.

2.2.7 Overexpression of TRAF4 RNA does not visibly rescue the TRAF4B MO knockdown phenotype

One way to test if a morpholino is specific, is to knockdown a protein-of-interest with the MO and then replace the protein with synthetic RNA. In many cases, this will repair the phenotype to something very similar to an untreated embryo. Here TRAF4A RNA was titrated at three doses and co-injected with 30 ng of the TRAF4B MO to test if exogenous TRAF4A RNA could rescue the TRAF4B knockdown phenotype (fig 2.11). Embryos were injected in the marginal zone at the two-cell stage and embryos were incubated until tail bud stage 32. A return to more normal looking development was not seen in any of the injection groups. TRAF4A overexpression alone lead to deformed embryos with disrupted convergence and extension movements and open blastopores. In addition, anterior features became smooth and rounded. When TRAF4A RNA and the TRAF4B MO were co-injected, all groups were more severely deformed than the TRAF4A overexpression alone. The co-injected embryos contained a mixture of embryos that lacked distinct anterior structures similar to TRAF4A RNA overexpression, and embryos with open blastopores and short torsos similar to TRAF4B MO knockdown. These results show that exogenous expression of TRAF4A was not able to rescue TRAF4B knockdown.

2.2.8 Overexpression of TRAF4 leads to anterior defects

In order to explore why exogenous expression of TRAF4 RNA was not able to rescue TRAF4B knockdown, the phenotype of TRAF4 RNA overexpression alone was investigated.

TRAF4A RNA was injected at 1 ng, 2 ng and 4 ng into the marginal zone of two-cell stage embryos and incubated until stage 35. At all doses injected, the embryos appeared unhealthy. Many had ill-defined anterior structures, and some were missing eyes as well as having a smaller cement gland (Fig. 2.12). Deformities are noticeable at 1 ng, and become more common as the dose of TRAF4 increases. Therefore, TRAF4A RNA overexpression is creating a phenotype and may not be suited to a phenotypic rescue.

2.3 Discussion

2.3.1 TRAF4A may be closer to a TRAF4 diploid predecessor

Comparison of the *X. laevis* homeologs of TRAF4 to the single TRAF4 in *X. tropicalis* may shed some light on any divergence that has occurred between the *X. laevis* homeologs, and possibly point to one homeolog being more similar to a diploid precursor. More similarity to a diploid precursor may suggest that a homeologs retains more of the functions of the diploid version of TRAF4. Therefore, the mRNA sequence of *X. tropicalis* TRAF4 and the two TRAF4 homeologs of *X. laevis* were compared through a nucleotide alignment. In order to setup an alignment that fairly assesses the identity between sequences, sequences of equal length were used in order to give more consistent results. When sequences differ in length, the percent identity can drop significantly even though the sequence that overlaps contains 100% identity. Each alignment contained the same length of nucleotides from each gene aligned, making differences and similarities more apparent. The 5' UTR alignment contains the first 140 bases of the 5' UTRs, and as the average 5' UTR in humans is 210 bases long, and in other vertebrates the average is 164 bases, there is a chance that most of the 5' UTR sequence is present in the alignment (Mignone et al., 2002). The 5' UTR alignment of the three genes showed TRAF4A to be much more similar to *X. Tropicalis* than to TRAF4B. Knowing that 5' UTRs contain motifs that can regulate the rate of translation (Mignone et al., 2002), the homeologs sharing 36.6% identity opens the possibility that TRAF4A and TRAF4B could display great differences in their translational regulation and protein abundance. The rate of translation could be tested in vitro and compared between TRAF4A and TRAF4B in order to answer the question of is there a homeolog that is more likely to be translated. However, blotting for endogenous protein would most likely stain both homeologs due to their shared sequence identity (96.17% for the protein sequences of TRAF4A and TRAF4B)(Fig. 2.4).

The coding sequence and the 3' UTR alignments showed TRAF4A to be just slightly more similar to TRAF4B than to *tropicalis*. The coding sequence shares 93.984% identity and the 3' UTR shares 80.3% identity. The coding sequence of TRAF4A and TRAF4B shares the highest identity, resulting in 18 amino acid changes within the TRAF4 protein. These amino acid changes do not occur within known sites necessary for domain function. However, this does not rule out that the homeologs have differing functions, as there may be residues discovered in

the future that play important roles in TRAF4 function. With 80% identity shared in the 3' UTR there is the possibility that mRNA localization signals have diverged, however, in situ staining suggests that expression patterns within the developing embryo are highly similar for the two homeologs (Fig 2.5) (Kalkan et al., 2009).

These data suggest that the greatest amount of divergence has taken place in the 5' UTR of TRAF4B, bringing up the possibility that translation of the two homeologs is regulated differently.

2.3.2 TRAF4 is expressed within the developing ectoderm

Untreated *Xenopus laevis* embryos were examined for TRAF4B expression using in situ hybridization and RT-PCR. Creation of a TRAF4B specific in situ probe was necessary to visualize TRAF4B expression during early development. To do so, a probe was created using a region of the TRAF4B 3' UTR published sequence. The TRAF4B 3' UTR extends for 2,738 bases past the end of the published TRAF4A 3' UTR (Fig. 2.1A). However, there is the possibility that the TRAF4A 3'UTR may be longer than what is published. The identity for the TRAF4A and TRAF4B 3' UTR using 900 bases of each is 80%. The possibility exists that the TRAF4B probe may be able to bind and stain TRAF4A. It is possible to determine the actual 3' UTR length and sequence can be determined by using 3' RACE (Rapid Amplification of cDNA Ends) to polymerize the TRAF4A 3' UTR starting from the poly-A tail and polymerizing towards the 5' end.

The TRAF4B probe gives an expression pattern similar to the TRAF4A ORF probe used by Kalkan et al., 2009, where TRAF4 is located in the enveloping ectoderm, and later in the neural ectoderm and anterior structures. A similar expression pattern is not surprising as the high identity of the ORF (94%) is likely to result in the ORF probe staining both homeologs.

In situ hybridization for TRAF4B (Fig. 2.5) gave a similar pattern to previous work by Kalkan et al., 2009, where they used an in situ probe complementary to the ORF of TRAF4A (Kalkan et al., 2009). Due to a 94% sequence identity in the open reading frame, this probe was predicted to bind to both homeologs. However the two in situ experiments did differ slightly. Similar to the in situ results by Kalkan et al., 2009, the TRAF4B probed blastula showed strong staining in the animal pole, however, the gastrula, did not give a strong band of staining

surrounding the blastopore lip as the TRAF4A ORF probe did. However, the entire ectoderm stained with the B probe, similar to TRAF4A ORF probe. The early neurula was previously reported to have staining in the cranial neural crest and cement gland. The TRAF4B probe gave darker staining in the cement gland and the neural plate, but did not stain the cranial neural crest as clearly. Stage 22 TRAF4B probed embryos, like previously reported stage 23 TRAF4A ORF probe embryos, show staining in anterior structures, along the spinal cord, and in posterior structures, but leave the ventral side of the embryo unstained.

When TRAF4 is knocked out in mice, tracheal narrowing defects are seen (Shiels et al., 2000). Some of these mice make wheezing sounds, and six out of nine wheezing mice showed lung inflammation. TRAF4 expression in these mice was seen in the first, second and third brachial arches, which are fated to become the bones of the jaw, the hyoid bone and pharyngeal structures. TRAF4 is also seen in the epithelium of the trachea. Also in mice, TRAF4 expression is found throughout embryonic development and can be seen more specifically throughout neurogenesis (Masson et al., 1998). TRAF4 is seen in the brain and spinal cord, and also in the facial and dorsal root ganglia. TRAF4 protein is also strongly expressed in the basal cells along the basement membrane of epithelium cells throughout the body (Krajewska et al., 1998). Additionally in mice, TRAF4 is found in the developing nervous system, and in the adult hippocampus and olfactory bulb, two regions known to contain multipotent cells (Masson et al., 1998). However, in these studies TRAF4 expression was not explored prior to neural tube closure and is not available to be compared with the early embryonic staining of *X. laevis*.

In addition to in situ hybridization, which visualizes expression patterns, TRAF4 homeolog transcript levels were measured in isolated ectoderm using RT-PCR (fig 2.7). In all stages tested, from blastula to mid-neurula, the TRAF4A transcript is at least 5-fold more prevalent than TRAF4B. RT-PCR data showed the TRAF4A transcript to be expressed at 5- to 47-fold higher levels than TRAF4B. This difference in transcript abundance may account for the fainter in situ staining seen with the TRAF4B probe than was seen for the TRAF4A ORF probe.

One concern in interpreting the RT-PCR data was that if the TRAF4 homeolog primers had different amplification efficiencies, the data would be skewed in favor of the primer set with the higher efficiency. The amplification efficiency for TRAF4A was 1.822 and for TRAF4B

1.824 (where 1 equals no amplification and 2 is a 100% doubling)(Ruijter et al., 2009b). In light of the facts that the two amplification efficiencies are very similar, and the TRAF4B primer set has the higher amplification efficiency, falsely high initial cDNA concentrations of TRAF4A do not seem likely.

2.3.3 The TRAF4B MO gives a more severe phenotype of open blastopores, and deformed anterior and posterior structures.

In order to show that the TRAF4A MO and TRAF4B MO are unique sequences, the TRAF4A MO sequence and TRAF4B MO sequence were aligned (Fig. 2.1). The sequences share eight common bases spread out along the 25 base oligonucleotide. The longest stretch of common sequence is three bases long. As 15 sequential bases are needed for specific binding, these two morpholino sequences are unlikely to bind the other TRAF4 homeolog non-specifically. Additionally, an alignment of the 5' UTR of the TRAF4A and TRAF4B transcripts show that the 5' UTRs share little homology (Fig. 2.10).

In order to examine how TRAF4 knockdown affects the developing embryo, I first tested whether one TRAF4 homeolog MO or a mixture of TRAF4 homeolog MOs would be most effective at knocking down TRAF4 (Fig. 2.7, 2.8). At the early tail bud stage, embryos injected with the TRAF4A MO at 50 ng, the TRAF4B MO at 25 ng and 50 ng displayed severe developmental defects, which included open blastopores, incomplete convergence and extension movements, ill-defined anterior structures, such as missing eyes, and a lack of defined posterior structures (Fig. 2.7). However, at 25 ng, injection of the TRAF4A morpholino did not give a noticeable phenotype. These embryos have defined anterior structures, such as eyes, cement glands and a ridge along the dorsal side of the trunk leading to the tip of the tail. Thus, the TRAF4B MO gave a more severe phenotype than the TRAF4A MO at an equivalent dose, making the TRAF4B MO a more potent tool for studying TRAF4 knockdown.

Deformities seen in the knockdown phenotype match the expression pattern of TRAF4, with defects being seen in anterior and posterior tissues. There may be two effects being observed in the tail bud stage phenotype, first the effects of inefficient gastrulation resulting in an open blastopore, and second, the knockdown of TRAF4 in the developing nervous system leading to a lack of defined neural and anterior structures.

To test if a more complete knockdown of TRAF4 could be achieved, I injected a combination of the TRAF4A and TRAF4B morpholinos at different ratios and examined the

knockdown phenotypes (Fig. 2.9). Combinations of TRAF4A and TRAF4B give a severe phenotype, however they are not more severe than injection of TRAF4B alone. It is interesting to note that addition of TRAF4A to TRAF4B does result in a more severe phenotype than the same dose of TRAF4B alone.

In light of the fact that the TRAF4B MO gives a more severe phenotype, I questioned if the greater penetrance of the TRAF4B MO is a result of the TRAF4B homeolog being more prevalent during development. However, TRAF4A transcripts are more abundant than TRAF4B from stage 7 (pre-zygotic transcription) through stage 20 (mid-neurula), suggesting that this is not the case (Fig. 2.6). There are a few possibilities to explain why the TRAF4B MO gives a more severe phenotype: the TRAF4B MO may be more effective at blocking translation, or the TRAF4B transcript may be preferentially translated.

The translation blocking efficiency of the MOs can be tested through a luciferase assay, where the 5'UTR containing the morpholino binding sequence and the beginning of the open reading frame are fused in frame with luciferase (Kamachi et al., 2008). Binding of the morpholino to the 5'UTR-luciferase reporter transcript results in a decrease in luciferase translation, which can be measured in a luminometer as a decrease in light emitted from luciferase (Promega Corporation, 2014).

Whether the TRAF4B transcript is being preferentially translated could also be tested through a reporter system. Directly testing translation through a western blot would not be feasible due to the two homeologs sharing 96% identity at the protein level (Kalkan et al., 2009). Instead, a luciferase assay could also be used to test if one transcript is being preferentially translated. In this case, the 5' UTR and 3' UTR would be needed in the luciferase fusion construct as most translational control elements are located in the untranslated regions (Wilkie et al., 2003).

2.3.4 The TRAF4B knockdown phenotype is not rescued by overexpression of TRAF4A RNA

Traditionally, morpholino specificity has been tested through rescue of the knockdown phenotype with a MO resistant version of the target transcript. The logic being that if the morpholino is reducing protein levels, addition of MO-resistant RNA will replace the protein and

restore normal development. Here TRAF4A RNA was titrated at three doses and co-injected with 30 ng of the TRAF4B MO to test if exogenous TRAF4 RNA could rescue the TRAF4B knockdown phenotype (fig 2.11). As the TRAF4A 5'UTR does not contain the TRAF4B MO sequence, it is naturally resistant to TRAF4B MO binding, (shown by Kalkan et al., 2009). However, titration of TRAF4A RNA at 1 ng, 2 ng or 4 ng per embryo did not rescue the phenotype caused by 30 ng of TRAF4B knockdown. On closer examination, we see that TRAF4A overexpression alone also results in deformed embryos (Fig. 2.12). Therefore, rescue with TRAF4 RNA may be unlikely, due to the teratogenic effects of TRAF4A overexpression.

However, clues can be gained as to the specificity of the morpholinos through injection of a combination of morpholinos at doses that do not give phenotypes when injected individually. In figure 2.7, 25 ng of TRAF4A morpholino does not give a phenotype, and in figure 2.10, we see that 8 ng of TRAF4B MO also does not give a phenotype. However, when 8 ng of TRAF4B MO and 8 ng of TRAF4A are mixed together there is a knockdown phenotype, which suggests that the two morpholinos are knocking down TRAF4, or are at least functioning in the same pathway. This phenotype becomes more prominent when TRAF4A is increased to 16 ng, even though a phenotype is not seen at 25 ng of TRAF4A alone. Since two subthreshold MO doses result in a phenotype similar to the phenotype achieved with a single morpholino, the phenotype seen when mixing the two MOs is most likely due to the combined knockdown of TRAF4. However, it is also possible that the MOs are knocking down proteins within the same pathway. However, this is less likely than the MOs knocking down the two homeologs of TRAF4.

A

Gene Name	Species	Accession	Length in nucleotides			
			5' UTR	Coding Sequence	3' UTR	Total length
TRAF4	X. *tropicalis*	NM_001005074.1	229	1413	977	2619
TRAF4A	X. *laevis*	NM_001094032.1	178	1413	941	2532
TRAF4B	X. *laevis*	NM_001093069.1	139	1413	3679	5232

B

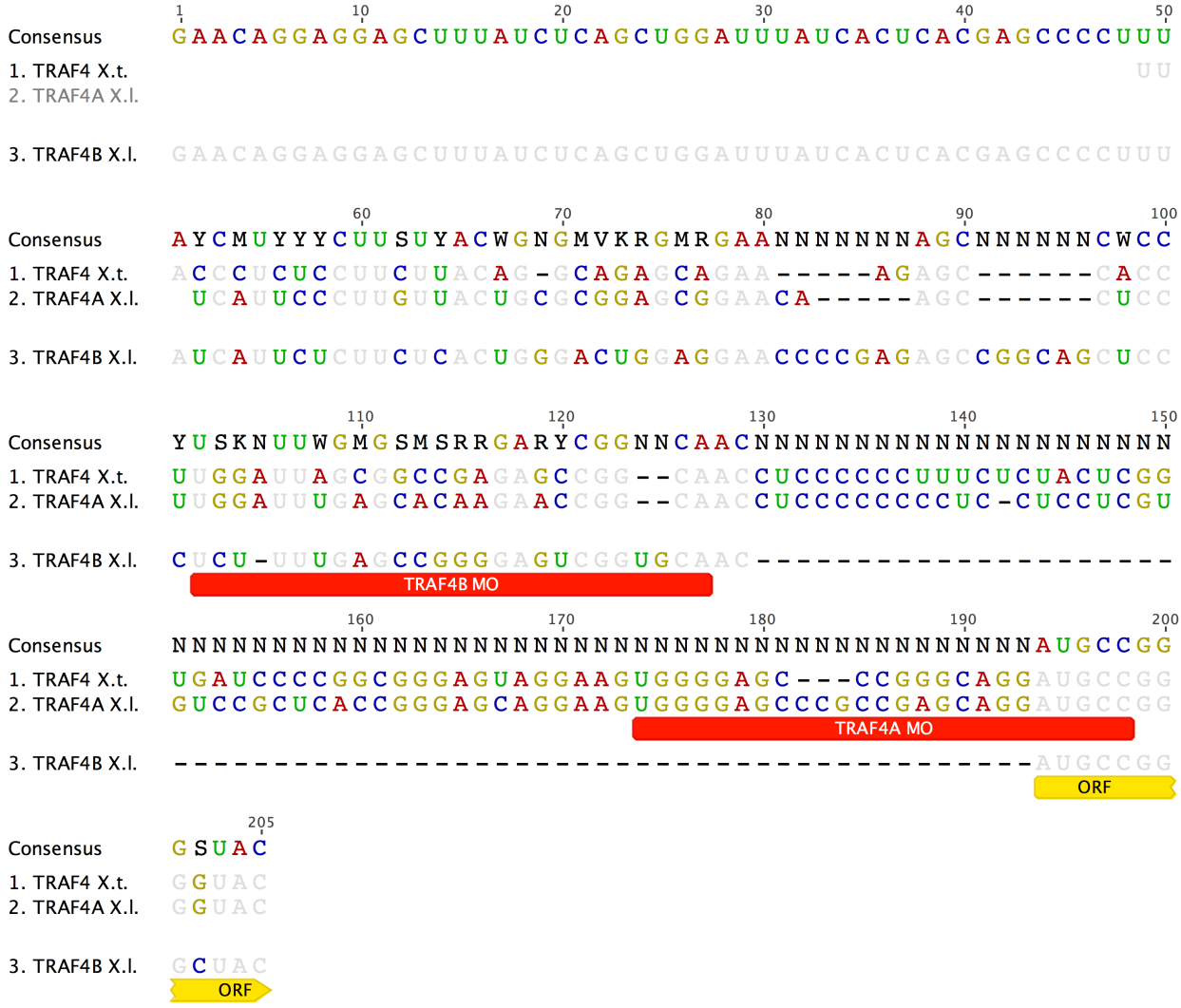

C

	TRAF4 *X.*t.	TRAF4A *X.*l.	TRAF4B *X.*l.
TRAF4 *X.*t.		73.427%	35.065%
TRAF4A *X.*l.	73.427%		36.601%
TRAF4B *X.*l.	35.065%	36.601%	

Figure 2.1 | Alignment of the 5' UTR of *Xenopus tropicalis* and *Xenopus laevis* TRAF4. 138 bases upstream and 12 bases downstream of the transcriptional start site were used to compare the similarity of *tropicalis* and *laevis* TRAF4. Bases that differ are colored by base. (**A**) Table of TRAF4 sequences, their NCBI accession numbers and region lengths. (**B**) Alignment of *X. tropicalis* TRAF4 and *X. laevis* TRAF4A and TRAF4B show *tropicalis* TRAF4 and TRAF4A to share the most similarity, with a shared identity 73.437% (**C**). TRAF4B shares the least similarity with *tropicalis* and TRAF4A at 35.065% and 36.601% respectively. The nucleotide alignment and table of identities were created using Geneious version 8.1.

A

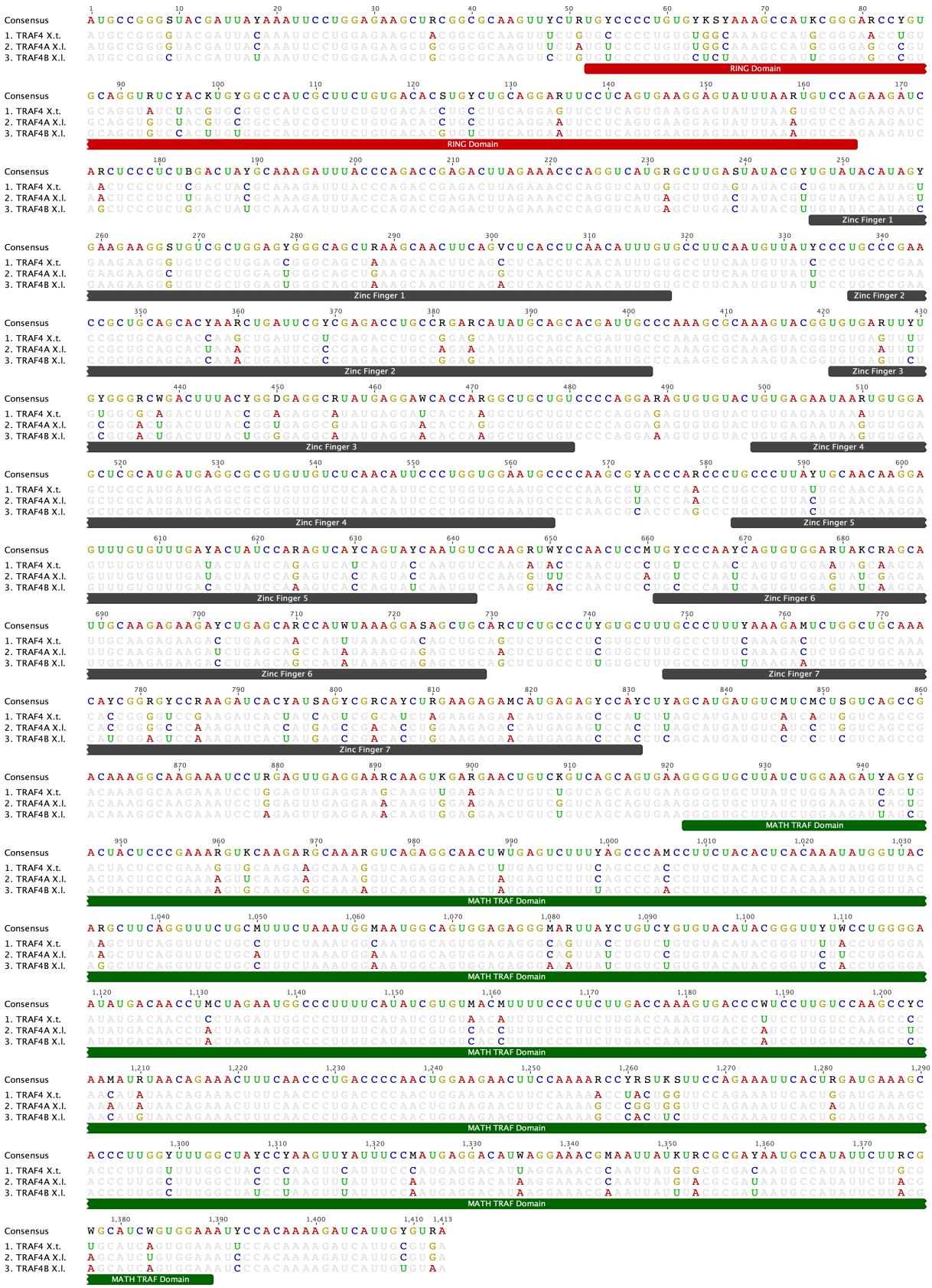
Consensus
1. TRAF4 X.t.
2. TRAF4A X.l.
3. TRAF4B X.l.
RING Domain
Zinc Finger 1
Zinc Finger 2
Zinc Finger 3
Zinc Finger 4
Zinc Finger 5
Zinc Finger 6
Zinc Finger 7
MATH TRAF Domain

B

	TRAF4 *X.*t.	TRAF4A *X.*l.	TRAF4B *X.*l.
TRAF4 *X.*t.	100%	93.489%	91.932%
TRAF4A *X.*l.	93.489%	100%	93.984%
TRAF4B *X.*l.	91.932%	93.984	100%

Figure 2.2 | Alignment of the coding sequences of *Xenopus tropicalis* and *Xenopus laevis* TRAF4. (**A**) Alignment of *X. tropicalis* TRAF4, *X. laevis* TRAF4 A and *X. laevis* TRAF4B with differences colored by base. (**B**) TRAF4A shares nearly as much identity with *tropicalis* TRAF4 as TRAF4B. The nucleotide alignment and table of identities were created using Geneious version 8.1.

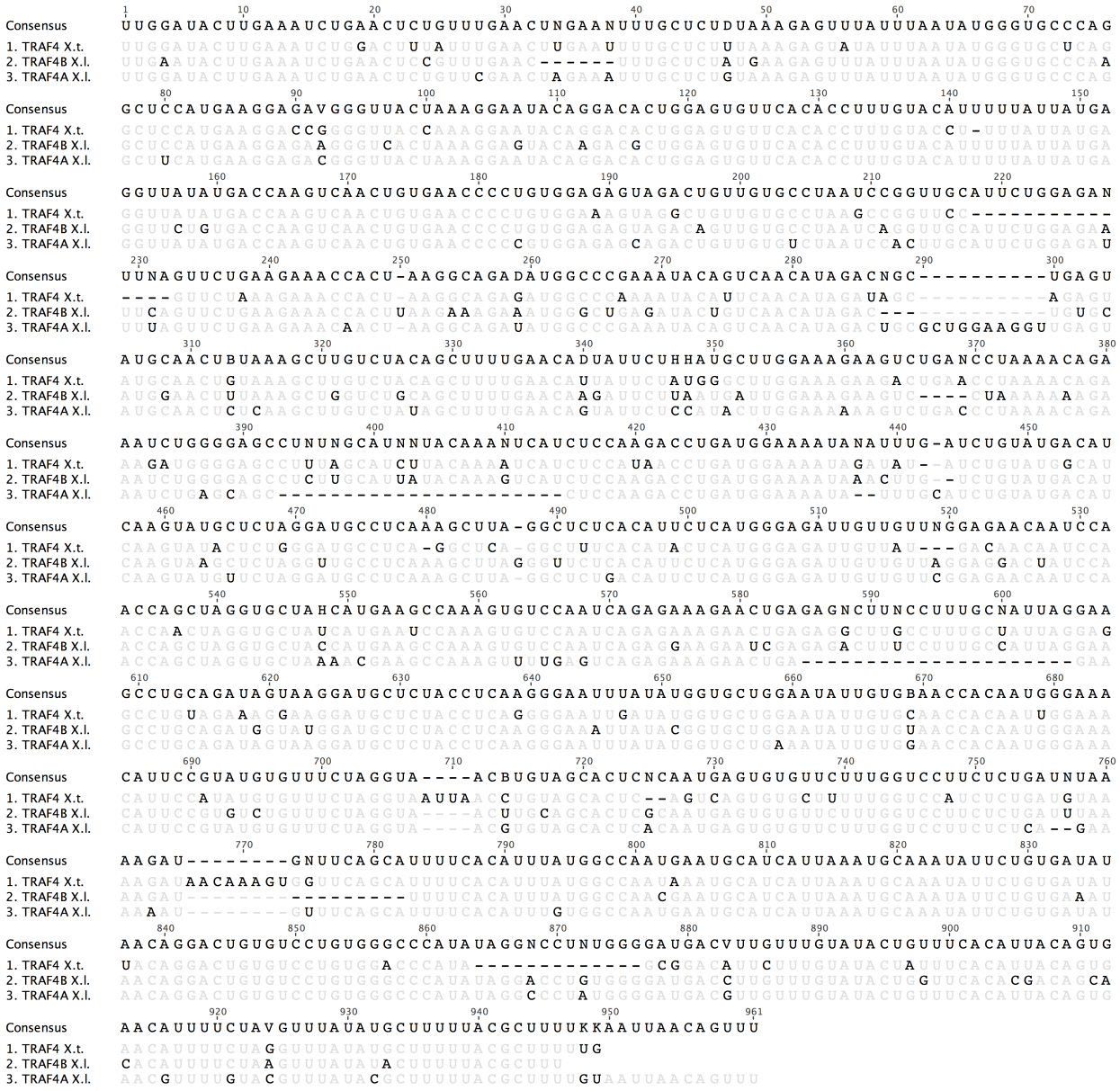

B

	TRAF4 *X.*t.	TRAF4A *X.*l.	TRAF4B *X.*l.
TRAF4 *X.*t.		78.075%	77.614%
TRAF4A *X.*l.	78.075%		80.300%
TRAF4B *X.*l.	77.614%	80.300%	

Figure 2.3 | Alignment of the 3' UTR of *Xenopus tropicalis* and *Xenopus laevis* TRAF4. This alignment uses the first 900 bases of each 3' UTR sequence. Identical bases are in light gray and differences are highlighted in black. Dashes mark gaps in the

sequence. (**A**) Differences in the sequence appear in black, whereas identical bases appear in gray. (**B**) *Tropicalis* TRAF4 is slightly more similar to TRAF4A than TRAF4B.

A

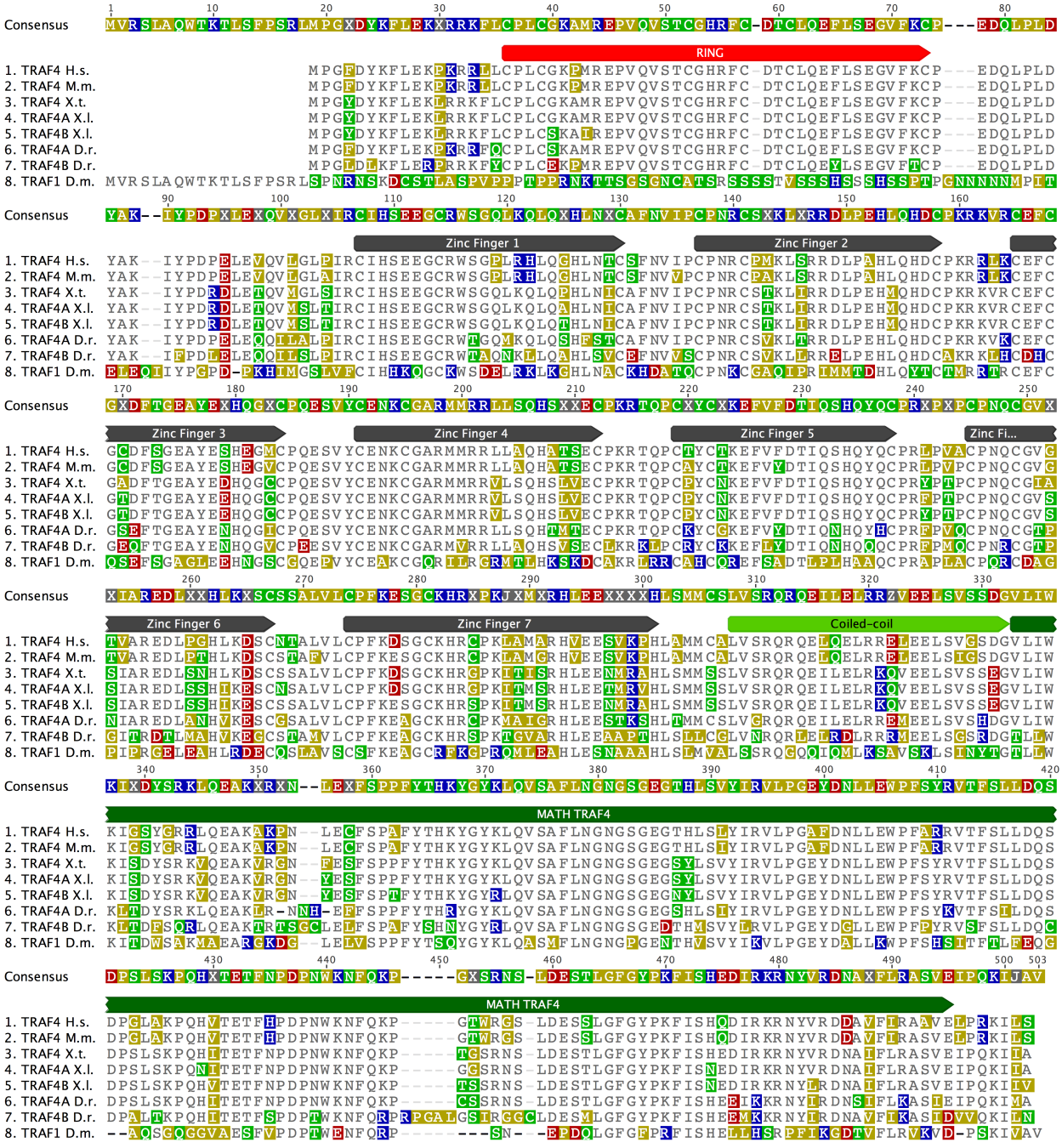
RING
Zinc Finger 1
Zinc Finger 2
Zinc Finger 3
Zinc Finger 4
Zinc Finger 5
Zinc Fi...
Zinc Finger 6
Zinc Finger 7
Coiled-coil
MATH TRAF4
MATH TRAF4
Consensus
1. TRAF4 H.s.
2. TRAF4 M.m.
3. TRAF4 X.t.
4. TRAF4A X.l.
5. TRAF4B X.l.
6. TRAF4A D.r.
7. TRAF4B D.r.
8. TRAF1 D.m.

B

	TRAF4 H.s.	TRAF4 M.m.	TRAF4 *X.*t.	TRAF4 A *X.*l.	TRAF4 B *X.*l.	TRAF4 A D.r.	TRAF4 B D.r.	TRAF1 D.m.
TRAF4 H.s.		96.809	77.872	77.660	76.596	76.483	67.155	39.496
TRAF4 M.m.	96.809		77.447	76.809	76.596	76.695	67.992	40.126
TRAF4 *X.*t.	77.872	77.447		95.957	94.894	81.568	67.364	41.387
TRAF4A *X.*l.	77.660	76.809	95.957		96.170	81.144	67.782	40.336
TRAF4B *X.*l.	76.596	76.596	94.894	96.170		80.508	67.992	40.336
TRAF4A D.r.	76.483	76.695	81.568	81.144	80.508		72.594	38.494
TRAF4B D.r.	67.155	67.992	67.364	67.782	67.992	72.594		37.190
TRAF1 D.m.	39.496	40.126	41.387	40.336	40.336	38.494	37.190	

Figure 2.4 | TRAF4 protein sequence alignment across six species. Comparison of eight TRAF4 protein sequences from fly to human. (**A**) TRAF4 contains a RING domain (excluding drosophila), seven zinc fingers and a c-terminal TRAF domain. Residues are colored by polarity: yellow – non-polar; green – polar, uncharged; red – polar, acidic; blue – polar, basic. (**B**) Percent identity between the eight TRAF4 protein sequences. The protein alignment and table of identities were created using Geneious version 8.1.

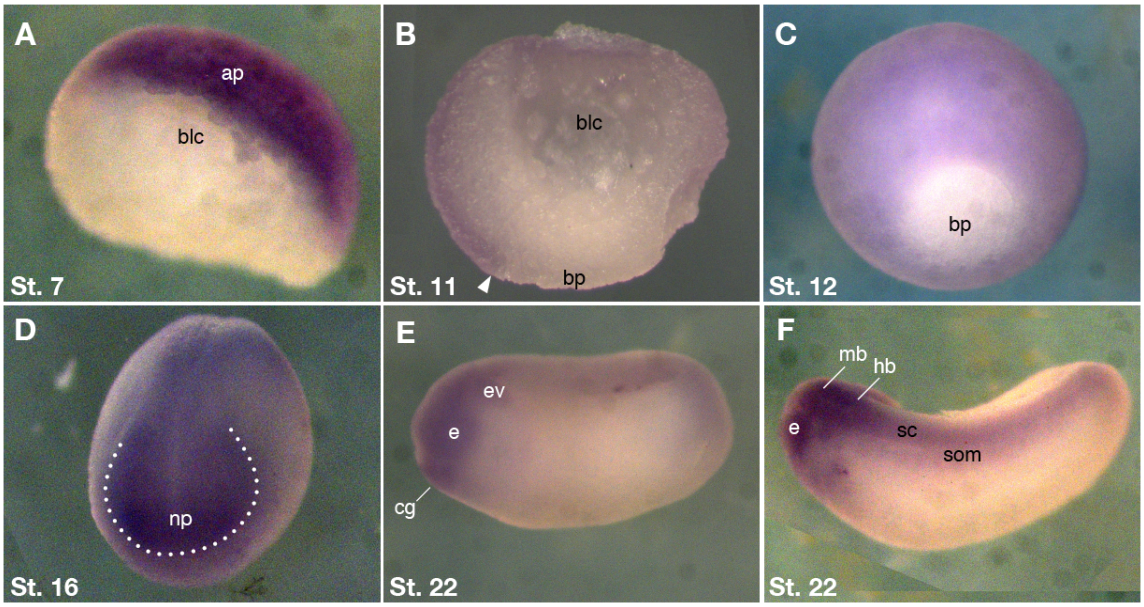

Figure 2.5 | TRAF4B expression during embryonic development (**A**) TRAF4B is expressed in the animal pole at stage 7. (**B**) TRAF4B can be seen in the ectoderm enveloping the outside of the embryo. The arrowhead denotes the blastopore lip. (**C**) TRAF4B staining is seen in the ectoderm, but not in the blastopore (bp). (**D**) TRAF4B is expressed in the neural plate and lighter staining is visible in the neural folds. The dotted line denotes the boundary between the neural plate and the neural folds. (**E**) TRAF4B staining is visible within anterior structures including the cement gland (cg), forebrain, midbrain, hindbrain, eye (e) and ear vesicle (ev). (**F**) Dark staining is seen in anterior structures including the eye, midbrain and hindbrain. TRAF4B expression is also visible in the spinal cord (sc) and somites (som).

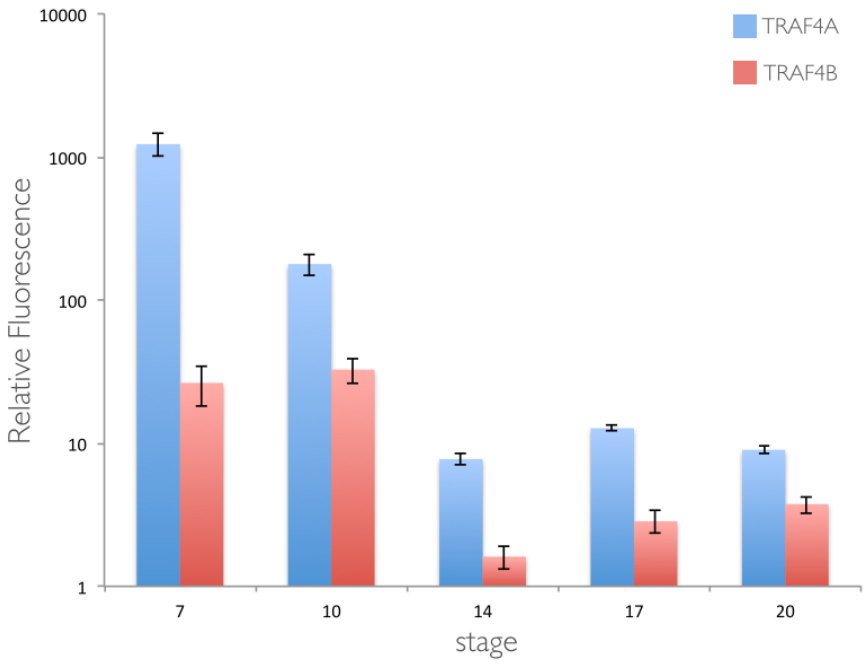

Figure 2.6| TRAF4A and TRAF4B homeolog expression in the early embryonic animal cap. Animal caps were incubated until the desired stage and then processed for RT-PCR. The expression of the TRAF4 homeologs was measured prior to the mid-blastula transition (stage 7), through the development of the neural tube (stage 20). The concentration of cDNA was measured in arbitrary fluorescent units.

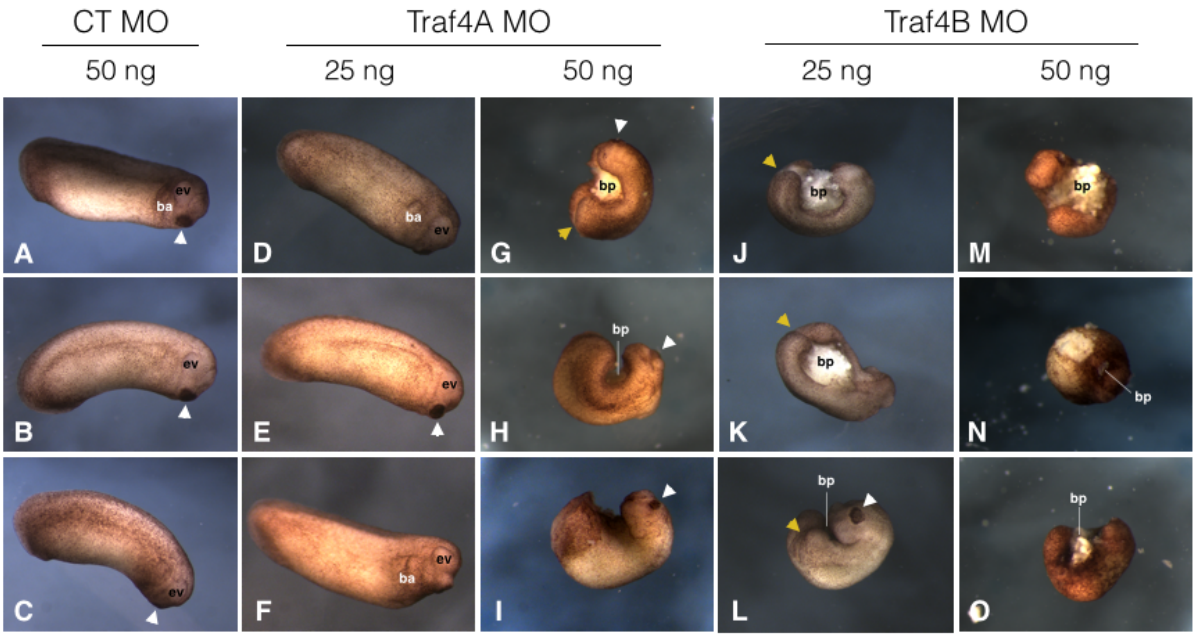

Figure 2.7 | Knockdown of TRAF4 results in an open blastopore and anterior defects. (**A-C**) Injection of a standard control morpholino resulted in normal stage 28 embryos. (**D-F**) 25 ng of TRAF4A MO gives embryos very similar to controls. (**G-I**) 50 ng of TRAF4A results in embryos with open blastopores, and anterior and posterior defects. (**J-L**) 25 ng of TRAF4B per embryo result in embryos very similar to 25 ng of TRAF4A. (**M-O**) 50 ng of TRAF4B MO result in embryos that are severely deformed, without discernable anterior or posterior features.

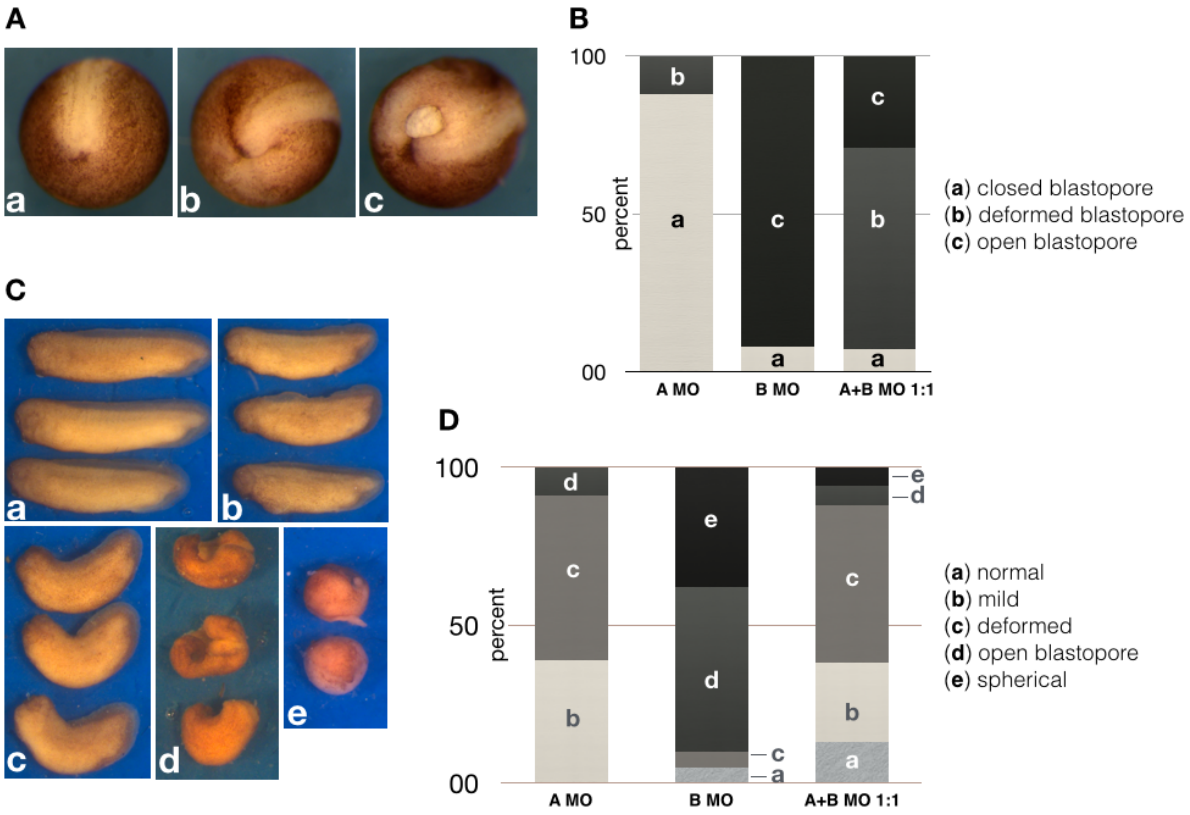

Figure 2.8 | Knockdown of TRAF4 leads to gastrulation defects and open blastopores. TRAF4A, TRAF4B or a combination of TRAF4A and B together were injected into the marginal zone of *Xenopus laevis* embryos at the two-cell stage. (**A**) Stage 13 morphant embryos can be classified into three phenotypes: closed blastopore (a), deformed blastopore (b), open blastopore (c). (**B**) Quantification of stage 13 embryos. Most TRAF4B MO injected embryos have open blastopores. (**C**) The embryos in A, were allowed to develop to stage 32. Morphants can be divided into five phenotypes: normal (a), mild (b), deformed (c), open blastopore (d), spherical (e). (**D**) Quantification of stage 32 phenotypes. TRAF4B MO injected embryos have more deformities than TRAF4A alone or mixed.

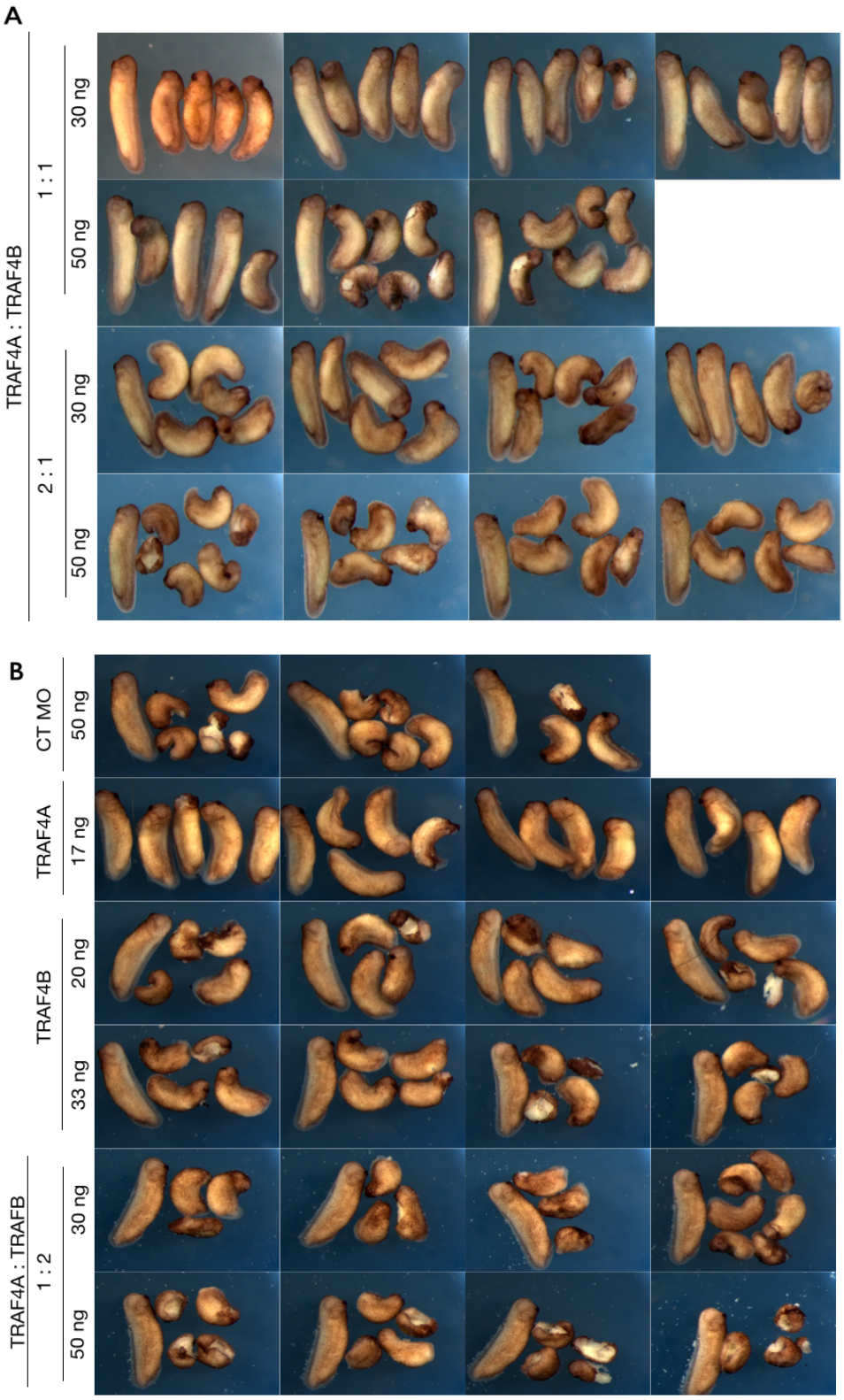

Figure 2.9 | Combinations of TRAF4A and TRAF4B do not give a more severe phenotype than TRAF4B alone. The TRAF4A and TRAF4B morpholino were mixed at different ratios and

different total doses in order to find a mixture that is most effective at TRAF4 knockdown as measured by the knockdown phenotype. The left-most embryo of each pane is a normally developing control. (**A**) TRAF4A and TRAFB in a 1:1 or 2:1 mixture show embryos that do not have open blastopores. (**B**) When TRAF4B is the primary morpholino, the phenotype becomes more severe. When the TRAF4B MO is injected in a 2:1 ratio, the A-P axis is shortened and defining anterior and posterior features become less defined.

Figure 2.10 | A mixture of TRAF4 morpholinos give a knockdown phenotype when injected at subthreshold doses. Embryos were injected in the marginal zone at the two-cell stage and incubated to tail bud stage 31. (A-C) Control embryos were injected with 50 ng of a standard control morpholino. (D-E) Embryos injected with a whole embryo dose of 8 ng of TRAF4B MO do show a phenotype. (G-I) Embryos injected with a mixture of 8 ng of TRAF4A MO and 8 ng of TRAF4B MO give a knockdown phenotype. (J-I) Increasing the dose of TRAF4A MO to 16 ng with 8 ng of TRAF4B MO results in a more severe phenotype. Neither 16 ng of TRAF4A MO or 8 ng of TRAF4B MO alone give a phenotype.

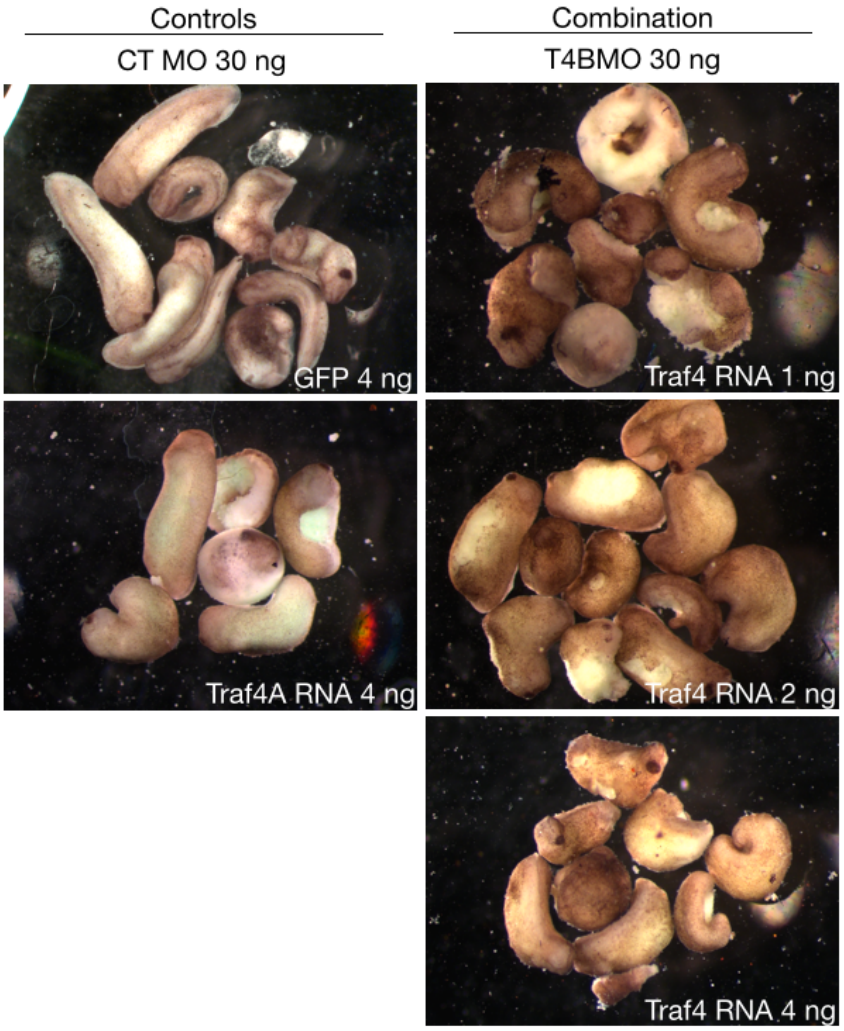

Figure 2.11 | Overexpression of TRAF4 RNA does not visibly rescue the TRAF4B MO knockdown phenotype. TRAF4B was knocked down with 30 ng of a TRAF4B MO into the two dorsal cells of the four-cell stage embryo. At doses of 1 ng through 4 ng of TRAF4 RNA, there is no visible rescue of the phenotype.

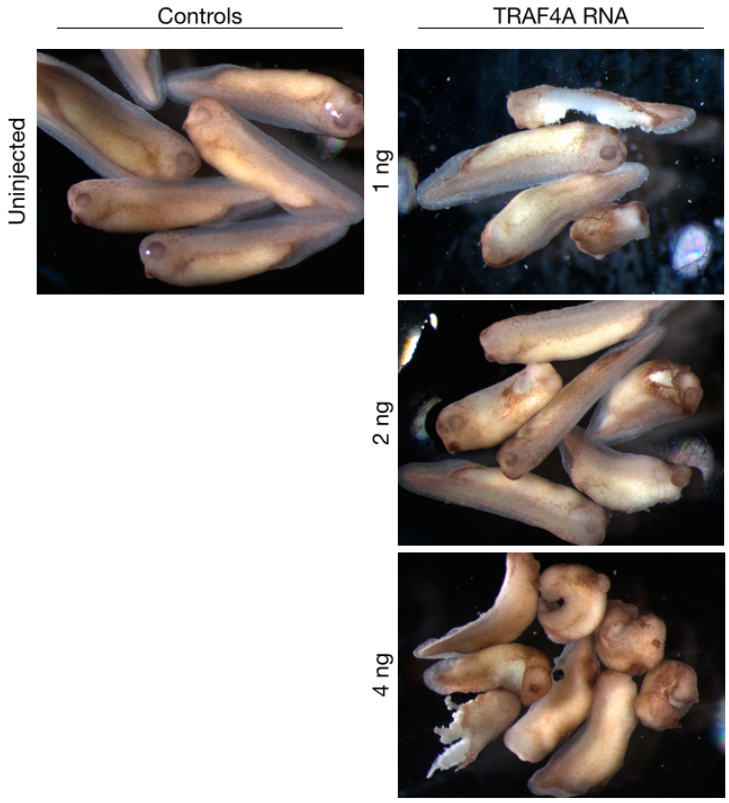

Figure 2.12| Overexpression of TRAF4 leads to anterior defects. TRAF4A RNA was injected into the two dorsal cells of the four-cell stage in increasing doses and imaged at tail bud stage 35. At 4 ng, anterior structures were less defined and embryos lack eyes, however, trunk length does not appear to be affected.

Chapter 3: Knockdown of TRAF4 reduces epidermal differentiation in animal caps

3.2 Results

3.2.1 Knockdown of TRAF4 results in a decrease in epidermal differentiation

Isolated animal caps when untreated become epidermal tissue. However, if BMP signaling is inhibited, the animal cap differentiates into neural tissue (Lamb et al., 1993; Zimmerman et al., 1996). The animal cap can be used to study epidermal differentiation by testing if manipulation of the animal cap alters the fate of the epidermis. In order to knockdown TRAF4B in the ectoderm, the TRAF4B MO was injected into the animal pole of the two-cell stage embryo in 12.5 ng, 25 ng or 37.5 ng per cell (25 ng, 50 ng or 75 ng per embryo). Control embryos were injected with 37.5 ng per cell making 75 ng per whole embryo of a random 25-mer morpholino control from Gene Tools. The random control MO is a mixture of random sequences, with a random base at each position of the oligonucleotide. This makes each oligonucleotide different and any off target binding occurs below the effective dose. Animal caps were isolated at stage 8 and incubated until mid to late neural fold stages (stage 16 to 18) when epidermal keratin is strongly expressed throughout the non-neural ectoderm. Four different sets of sibling embryos were used to isolate 12 to 18 animal caps per injection group. The collected caps were processed for RT-PCR and expression data was normalized to a housekeeping gene, either ODC or eEF1α.

As the dose of TRAF4B MO increased, the expression of epidermal keratin and BMP4 decreased (Fig. 3.1). At 75 ng per cap, the decrease in epidermal keratin expression becomes statistically significant with a ($p < 0.05$). Loss of epidermal keratin suggests that the ectoderm is losing epidermal characteristics. Knockdown of TRAF4B also resulted in a trending decrease in BMP4 expression. As BMP4 is essential for epidermal differentiation, this trending decrease also suggests that the ectoderm is no longer producing an epidermal fate. The decrease in these two markers support the hypothesis that TRAF4B is a positive regulator of BMP signaling, and is necessary for robust BMP signaling and differentiation of the epidermis.

3.2.2 Loss of TRAF4B results in expression of an early neural stem cell marker, Sox2

Regulation of BMP signaling is essential for patterning of the ectoderm, where ventrally located BMPs induce epidermis, and dorsally located inhibitors of BMP ligands block BMP signaling and allow for neural induction. When BMP signaling is inhibited in the presumptive ectoderm (the animal cap), neural tissue will be induced instead of epidermis. Therefore, if knockdown of TRAF4 is inhibiting BMP signaling, neural induction is expected to occur. I tested if knockdown of TRAF4 results in increased expression of the early neural stem cell marker Sox2. Embryos were injected with morpholino into the animal pole of each blastomere at the two-cell stage. Animal caps were isolated at stage 8 and incubated until mid to late neural fold stages (stage 16 to 18) when both epidermal and neural ectoderm are present. Control embryos were injected with 75 ng of a standard control morpholino and test groups were injected with either 25, 50 or 75 ng of TRAF4B MO. Uninjected whole embryos were used as a comparison for total embryonic expression. RT-PCR data was normalized to ODC and uninjected caps (not shown) were set to one.

As the dose of TRAF4B MO increased, Sox2 expression also increased, reaching statistical significance at 75 ng of TRAF4B MO (Fig. 3.2A). Figure 3.2B shows that injection of the TRAF4A morpholino gives Sox2 expression similar to the control morpholino, whereas injection of the TRAF4B MO gives much greater Sox2 induction. This also demonstrates that the TRAF4B morpholino is more effective at neuralizing the embryo.

3.2.3 Markers of differentiated neural tissue do not change as TRAF4 knockdown increases.

In order to test if TRAF4 knockdown is inducing neural tissue, I tested if markers of differentiated neural tissue are induced after loss of TRAF4. Embryos were injected with morpholino into the animal pole of each blastomere at the two-cell stage. Animal caps were isolated at stage 8 and incubated until mid to late neural fold stages (stage 16 to 18) when both epidermal and neural ectoderm are present (Fig. 3.3). Control embryos were injected with 75 ng of a standard control morpholino and test groups were injected with either 25, 50 or 75 ng of TRAF4B MO. Uninjected whole embryos were used as a comparison for total embryonic

expression. RT-PCR data was normalized to ODC and uninjected caps were set to one. NCAM, a marker of immature neurons, and XAG-1, a marker of the cement gland, did not increase as TRAF4 decreased, suggesting that TRAF4 knockdown using the B MO at 75ng is not sufficient for neural induction.

3.3 Discussion

3.3.1 Knockdown of TRAF4B results in a decrease in epidermal differentiation

If TRAF4 is a positive regulator of BMP signaling, then loss of TRAF4 would be predicted to interfere with the fate of BMP regulated tissues. Removal of the animal cap (the presumptive ectoderm) at pre-gastrula stages, and incubation until neurulation results in epidermal differentiation of the isolated cap, which requires BMP signaling. Previous studies by Kalkan et al., 2009, show that TRAF4 overexpression alone cannot increase expression of genes downstream of BMP. In addition, they show that addition of TRAF4 can reduce neural induction after the injection of a dominant-negative BMP receptor or injection of an extracellular BMP inhibitor. Therefore, I was interested in testing if TRAF4 knockdown alone could decrease BMP signaling under endogenous conditions. Here I show that knockdown of TRAF4 results in a decrease in markers of epidermis (Fig. 3.1). When embryos are injected with a dose of 75ng of TRAF4B morpholino, epidermal keratin is significantly reduced and BMP4 shows a consistent downward trend. As robust BMP signaling is needed for epidermal differentiation, a loss of epidermal markers supports the hypothesis that TRAF4 plays a role in BMP signaling and the differentiation of the ectoderm.

3.3.2 Knockdown of TRAF4B results in expression of Sox2, but does not increase markers of more differentiated anterior structures.

Consistent with the loss of epidermal markers, increasing doses of TRAF4B morpholino result in increasing expression of Sox2. At 75 ng of TRAF4B MO per animal cap, Sox2 was significantly increased with a p-value of less than 0.05. As Sox2 is not expressed in the epidermal ectoderm, expression of Sox2 points to the loss of epidermal tissue and the beginning of neural induction. However, Sox2 is a marker of early neural differentiation and does not represent a committed neural fate. Instead, the presence of Sox2 alone denotes a shift from epidermis to a neural competent state (Wills et al., 2010). In addition, knockdown of TRAF4B, but not TRAF4A, results in the neuralization of the *Xenopus laevis* ectoderm as measured by Sox2 induction. Knockdown of TRAF4A induces Sox2 in a manner similar to the control morpholino, whereas the TRAF4B morpholino shows a large increase in Sox2 expression (figure

3.2B). This data, in addition to the phenotypic data, suggests that the TRAF4B MO gives greater knockdown effects.

As Sox2 is a marker of neural stem cells and does not necessarily denote a neural fate, markers of differentiated neural and anterior tissues were also tested. NCAM, marks the presence of neural induction (Kintner and Melton, 1987) and XAG-1 marks formation of the cement gland, the most anterior structure in the Xenopus embryo. In both cases, there was no increasing or decreasing trend and expression levels were similar to controls (Fig. 3.3). This data suggests that loss of TRAF4 is not sufficient for neural induction.

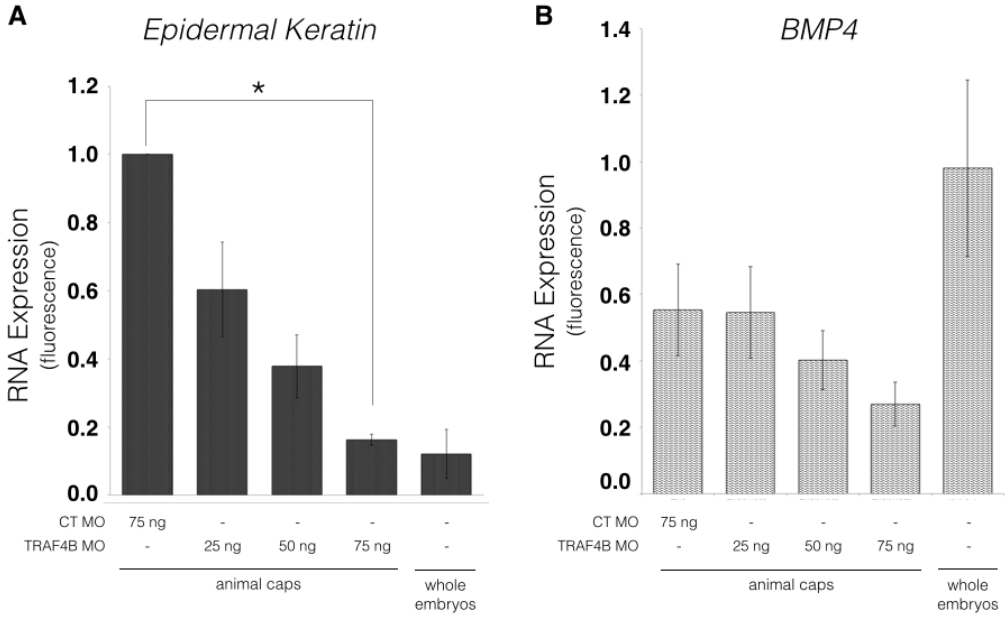

Figure 3.1 | **TRAF4B knockdown results in a loss of epidermal characteristics.** Embryos were injected with morpholino in the animal pole at the two-cell stage. Animal caps were cut and were tested for epidermal markers at mid to late neural fold stages (stages 16 to 18). (**A**) Epidermal keratin decreases as TRAF4B MO increases. At a TRAF4B MO dose of 75 ng, knockdown of epidermal keratin was significant lower than the control. (**B**) BMP4 expression decreases as TRAF4B MO increases.

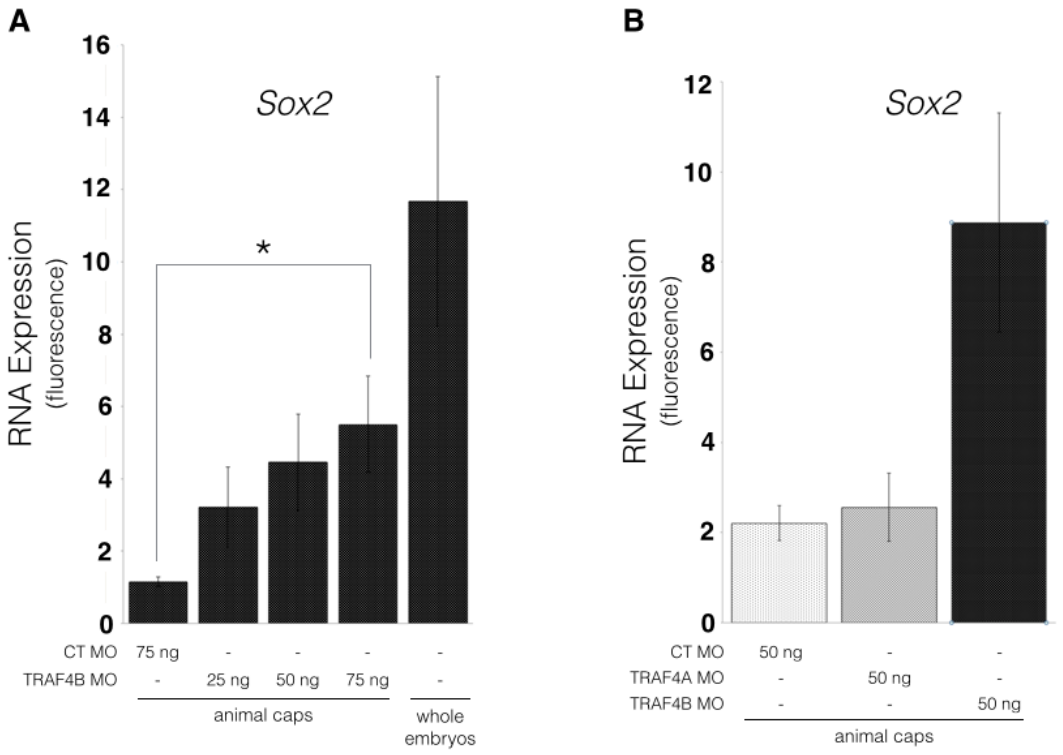

Figure 3.2| Knockdown of TRAF4B results in an increase in Sox2. Sox2 expression in stage 16 to 18 animal caps after injection of a TRAF4B morpholino. (**A**) Sox2 expression increases as TRAF4B knockdown increases. At 75 ng per embryo, the increase in Sox2 expression becomes statistically significant. (**B)** TRAF4 knockdown using homeolog specific morpholinos at the same dose gives differing induction of Sox2. At 50 ng, TRAF4A knockdown results in SOX2 expression similar to control levels, however, TRAF4B knockdown results in a strong induction of Sox2 expression.

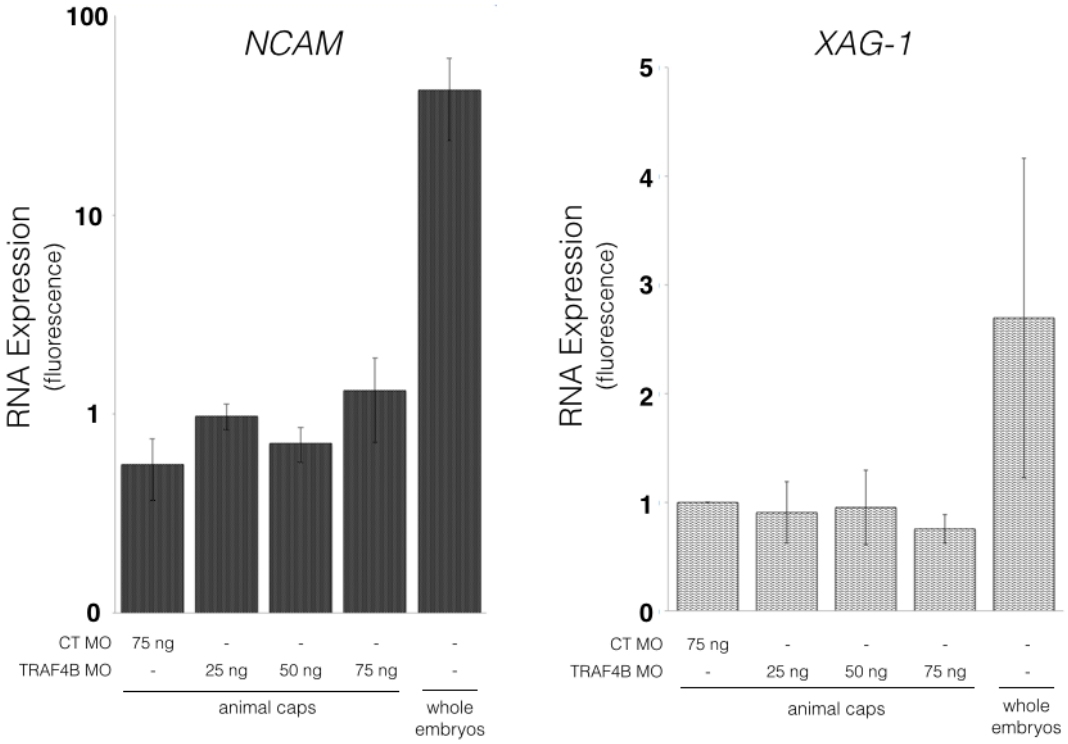

Figure 3.3 | Markers of differentiated neural tissue do not change as TRAF4 knockdown increases. Expression levels of markers of differentiated anterior tissue in the ectoderm at stages 16-18 after increasing doses of TRAF4B knockdown. (**A**) NCAM, a marker of immature neurons, does not show an increasing trend as TRAF4B knockdown increases. (**B**) XAG-1, a marker of the cement gland, does not show an increasing or decreasing trend as TRAF4B knockdown increases.

Chapter 4: TRAF4 likely participates in TGF-β by altering Smad activity

4.2 Results

4.2.1 Knockdown of TRAF4B allows embryos overexpressing Xenopus nodal-related 2 to regain the ability to gastrulate.

Previous studies have shown TRAF4 to influence Nodal and TGF-β signaling (Kalkan et al., 2009; Zhang et al., 2013). However, the effects of TRAF4 on early developmental processes have not been well studied. Here I show that knockdown of TRAF4 in vivo can attenuate the effects of Xnr2 overexpression. A mixture of 50 pg of Xnr2 RNA and 50 ng of morpholino was injected into the marginal zone of each blastomere of two-cell stage embryos and grown until the completion of gastrulation at stage 13. Control embryos completed gastrulation as shown by a closed blastopore (Fig. 4.1, white arrows). TRAF4 knockdown embryos exhibited delayed gastrulation, but were able to create a circular blastopore lip. Embryos overexpressing Xenopus nodal-related protein 2 (Xnr2) began to develop a blastopore lip (white arrowheads), but did not form a circular blastopore lip and did not exhibit movements of gastrulation. Embryos co-injected with Xnr2 and the TRAF4B morpholino regained the ability to create a circular, involuting blastopore. This phenotype suggests that the loss of TRAF4 decreases Nodal signaling, allowing the embryo to perform the movements of gastrulation.

Nodal signaling is essential for the induction and differentiation of the mesoderm, including the ability of the mesoderm to involute and gastrulate (Osada and Wright, 1999). However, overexpression of Nodal at high doses into the marginal zone of the early Xenopus embryo results in an expansion of the endoderm and a loss of gastrulation (Gritsman et al., 2000). If TRAF4 is a positive regulator of TGF-β signaling, then the loss of TRAF4 is expected to reduce TGF-β signaling activity. A decrease in TGF-β activation can be visualized in vivo with an embryo regaining the ability to gastrulate. I injected 50 pg of either GFP or Xenopus Nodal-Related 2 (Xnr2) RNA with 50 ng of a standard control or TRAF4B MO into the marginal zone of two-cell stage embryos. The embryos were then incubated at 18˚C and imaged at stage 13, which is the end of gastrulation as defined by a fully closed blastopore.

Control embryos injected with GFP and the standard control MO closed their blastopore at stage 13 (A-C). Embryos injected with GFP and the TRAF4B MO (D-F) displayed a delay in gastrulation, giving the appearance of a stage 11 embryo at stage 13. Embryos injected with Xnr2 and the control MO (G-I) failed to gastrulate or presented a blastopore lip more apically located than a blastopore lip occurring in a healthy stage 10 embryo. However, when Xnr2 and TRAF4B MO were co-injected (J-L), these Xnr2 injected embryos retained their ability to gastrulate. Regaining the ability to gastrulate in the presence of Xnr2 suggests that the loss of TRAF4 is dampening the effects Xnr2 overactivation.

4.2.2 Knockdown of TRAF4B allows embryos overexpressing BMP4 to regain the ability to gastrulate.

Induction of mesoderm occurs after Nodals released from the endoderm induce the tissue of the marginal zone to become mesoderm. A gradient of BMP activity is required for pattering the mesoderm into dorsal and ventral tissues. I tested if the loss of TRAF4 can rescue the effects of BMP overexpression (Fig. 4.2). Sibling embryos were injected in the marginal zone of each blastomere of the two-cell stage embryo. Control embryos were injected with 1.5 ng of GFP and 75 ng of the Gene Tools standard control morpholino (CCTCTTACCTCAGTTACAATTTATA). A BMP overexpression group was injected with 1.5 ng of BMP4 and 75 ng of the standard control MO, and a rescue group was injected with 1.5 ng of BMP4 RNA and 75 ng of TRAF4B MO. The embryos were incubated at 18˚C until the control embryos reached stage 23, and then imaged under a dissecting microscope.

Control embryos (Fig3.3, A-C) developed normally to stage 23, and displayed well defined anterior structures, a cement gland and gills, and a ventral ridge (NIEUWKOOP and FABER, 1956). Embryos injected with BMP4 RNA failed to gastrulate (D-F). The embryos retained the coloring of a pre-gastrula embryo with a dark animal pole and light yellow ventral pole. The embryos remained mostly spherical except for an outward protrusion on the ventral side of the embryo. There were no visible signs of gastrulation, which would be marked by a dark dorsal lip or blastopore ring, nor were there any sign of completed gastrulation, which would be marked by a closed blastopore and dark animal pole coloring surrounding the entire embryo as the ectoderm encapsulates the embryo. However, embryos co-injected with BMP4 RNA and the TRAF4B MO regain the ability to gastrulate (G-I). Co-injected embryos give the appearance of

roughly stage 11 embryos despite sibling control embryos being at stage 23. The blastopore developed into a full ring and is slightly protruding suggesting that the embryo may be exogastrulating. The appearance of a blastopore ring suggests that the loss of TRAF4B limits BMP4 activity enough to restore gastrulation.

4.2.3 pSmad1 intensity decreases with TRAF4B knockdown

In order to test if BMP activity is affected by the loss of TRAF4, a western blot for Smad1 with an activating c-terminal phosphorylation referred to as pSmad1 was performed (Fig. 4.3). Reagents were injected according to the table 3.1. Reagents were injected into the marginal zone of the two-cell stage embryo and embryos were incubated until gastrulation (stage 12) when a western blot was performed. Fluorescence was then detected and measured using a Li-Cor Odyssey fluorescent scanner. The TRAF4B MO alone gave pSmad1 levels slightly less than uninjected embryos. BMP4 injected alone, as expected, gave a sharp increase in pSmad1 as BMP4 activates the BMP pathway and Smad1. Co-injection of BMP4 and TRAF4 MO gave nearly a 40% decrease in pSmad1 levels. This data suggests that TRAF4 knockdown is indeed decreasing BMP signaling, and that this effect is occurring upstream of pSmad1 activating phosphorylation.

4.2.4 Expression of mesoderm markers after co-injection of Xnr2 and a TRAF4B MO

In order to test if TRAF4 plays a role in mesoderm induction, animal caps were injected with a mesoderm inducer alone or a mesoderm inducer with a TRAF4 MO. RT-PCR was then used to measure the relative expression of mesoderm markers. Embryos were injected in the animal pole of each blastomere of the two-cell stage. Embryos were incubated until stage 8 when animal caps were removed and incubated until the end of gastrulation, stage 13. Reagents were injected into the animal cap according to figure 4.2. Markers of dorsal mesoderm Muscle Actin, Chordin and Cerberus displayed a pattern of strong induction after Xnr2 overexpression, little induction after injection of the control or TRAF4B alone, and reduced expression when Xnr2 and TRAF4B MO were co-injected. These three markers suggest that loss of TRAF4 is negatively affecting mesoderm induction. However, other markers of mesoderm induction,

Brachyury, Goosecoid, Mix.2, MyoD and Xhox3, give a different pattern. They increase when Xnr2 is overexpressed and TRAF4B is knocked down. This suggests that TRAF4 may have a second function within the organizer and mesoderm.

4.3 Discussion

4.3.1 Knockdown of TRAF4B rescues gastrulation in embryos overexpressing Xnr2

Overexpression of 5 pg of Xnr2 injected into the marginal zone of two-cell stage embryos result in stage 10 embryos that begin to form a dorsal lip, but are unable to bring the blastopore lip fully around to the vegetal half of the embryo by stage 13, when the blastopore is closed in untreated embryos. Embryos overexpressing Xnr2 are able to regain the ability to form a circular blastopore lip and perform gastrulation movements after co-injection of a TRAF4B morpholino. Regaining the ability to form a full blastopore lip and perform gastrulation movements suggests that loss of TRAF4B is decreasing Xnr2 signaling enough to allow for more normal development to proceed. However, gastrulation and normal development are not completely rescued.

4.3.2 Knockdown of TRAF4B allows embryos overexpressing BMP4 to regain the ability to gastrulate.

Previously published data showed that TRAF4 can reduce neural induction induced by a truncated BMP receptor or by the BMP inhibitor noggin (Kalkan et al., 2009). However, the effects of TRAF4 knockdown in the mesoderm were not well explored. One effect of overexpression of BMP4 is the lack of blastopore lip formation. Here I show that after BMP overexpression, knockdown of TRAF4 allows the blastopore lip to form and partially close (figure 3.4). Even so, BMP4/TRAF4B MO co-injected embryos were still gastrulating by stage 20, when the healthy embryo has completed gastrulation and the neural tube fully closed.

To test if TRAF4 is affecting BMP activity, pSmad1, the carrier of activated BMP signals from the membrane to the nucleus, was measured in response to TRAF4 knockdown (Fig. 4.3). As TRAF4 is hypothesized to potentiate BMP signaling, a loss of TRAF4 is expected to decrease pSmad1 levels. Indeed, a western blot of pSmad1 shows that knockdown of TRAF4 reduces pSmad1 levels by 40%. This suggests that TRAF4 does decrease BMP signaling and that loss of TRAF4 exerts its affect through Smad activation.

4.3.3 Co-injection of Xnr2 and a TRAF4B MO on mesoderm marker expression

Overexpression of Nodals into the animal cap induces the presumptive ectoderm to become mesodermal tissue. In order to test if TRAF4 is positively regulating Nodal signaling, Xnr2 was overexpressed and mesoderm was induced. Knock down of TRAF4B was not expected to induce markers of mesoderm, but did induce signaling to a greater degree than the control group. If TRAF4 is a positive regulator of Nodal signaling, then reduction of TRAF4 is predicted to reduce signaling and thereby reduce markers of mesoderm induction. Co-injection of Xnr2 and the TRAF4B MO result in a reduction of Muscle Actin, Chordin and Cerberus when compared to Xnr2 injection alone, pointing to a reduction in Nodal signaling. However, Brachyury, Goosecoid, Mix.2, MyoD and Xhox3 increased when TRAF4 was knocked down in the presence of Nodal overexpression.

This sharp increase in Goosecoid is similar to results seen by Zhu et al., 1999, where co-injection of Smad2, a nodal activator, and Smurf1, a BMP inhibitor, induced goosecoid only when co-expressed (Zhu et al., 1999). They suggest that inhibition of BMP signaling by Smurf1 enhances the sensitivity of animal caps to Smad2. It is possible that TRAF4 preferentially inhibits BMP signaling, allowing for enhanced sensitivity to Xnr2 and a sharp increase in goosecoid expression.

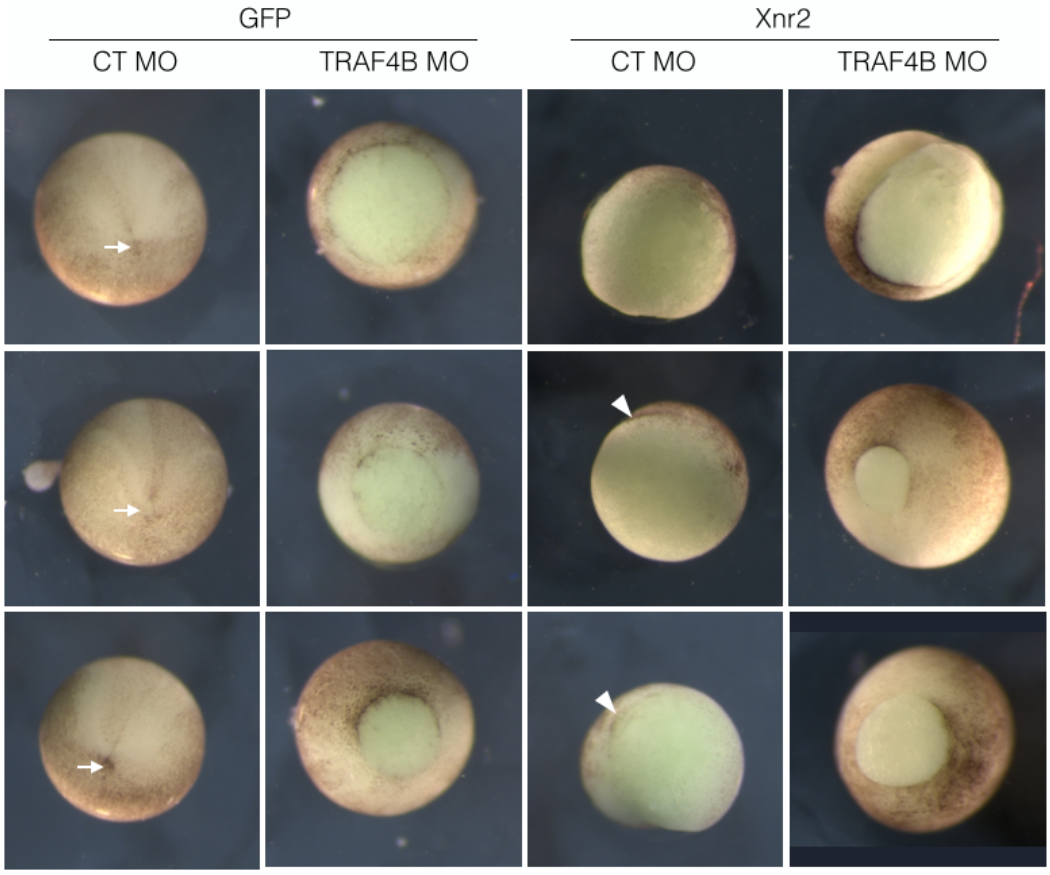

Figure 4.1 | Embryos overexpressing Nodal regain the ability to gastrulate after TRAF4 knockdown. Embryos were injected with reagents at the 2-cell stage and imaged at stage 13, which marks the end of gastrulation. White arrows mark the closed blastopore. Control embryos were injected with 50 ng of a standard control MO and 50 pg of GFP RNA. Embryos injected with 50 ng of TRAF4B MO and 5 pg of GFP exhibit delayed gastrulation. Embryos injected with 50 ng of a standard control MO and 5 pg of Xnr2 RNA form a blastopore lip (white arrowheads) that does not encompass the embryo. Embryos co-injected with 50 ng of TRAF4B MO and 5 pg of Xnr2 RNA form a blastopore and display movements of gastrulation.

	Control	Overexpression	Rescue
Control MO	75 ng	75 ng	
TRAF4B MO			75 ng
GFP RNA		1.5 ng	
BMP4 RNA	1.5 ng		1.5 ng

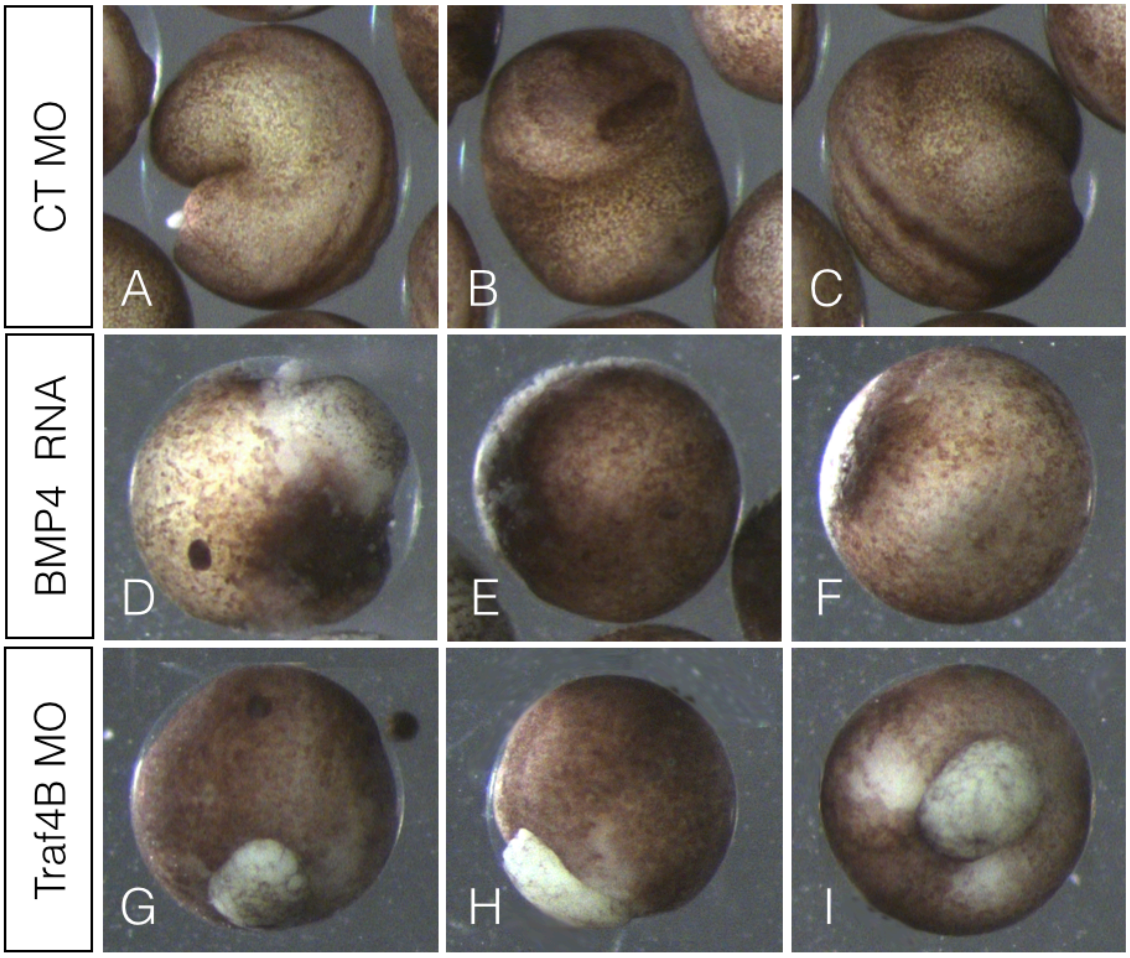

Figure 4.2| Embryos co-injected with BMP4 and TRAF4B MO regain the ability to gastrulate. Embryos injected with a standard control morpholino and imaged at stage 20 (**A-C**). Embryos injected with 1.5 ng of BMP4 do not gastrulate (**D-F**). Embryos co-injected with 1.5 ng BMP4 and 75 ng of TRAF4B form a blastopore and partially gastrulate (**G-I**).

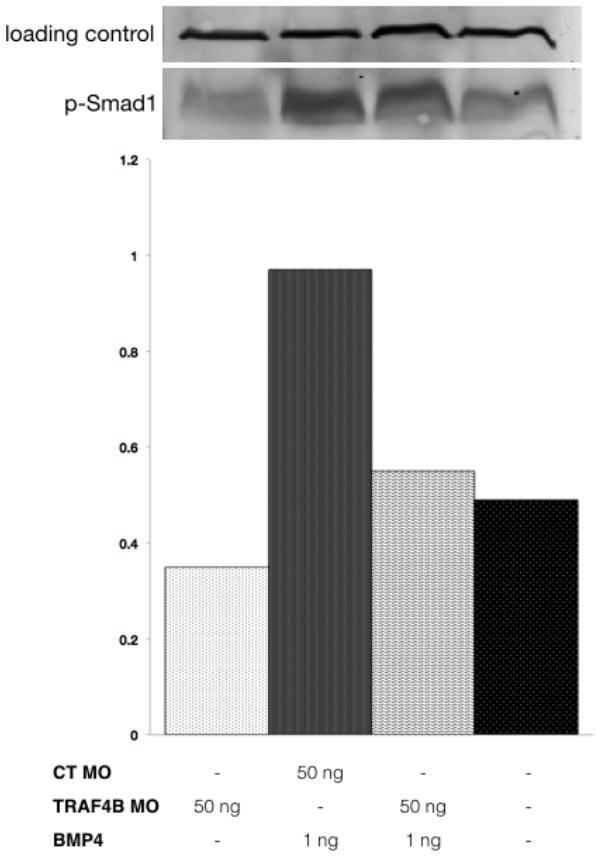

Figure 4.3| pSmad1 decreases with TRAF4B knockdown. Embryos were injected in the marginal zone at the two-cell stage according to the table below the graph. BMP4 injected embryos showed a spike in pSmad1 levels. Embryos injected with BMP4 and TRAF4B MO gave a decrease in pSmad1 levels.

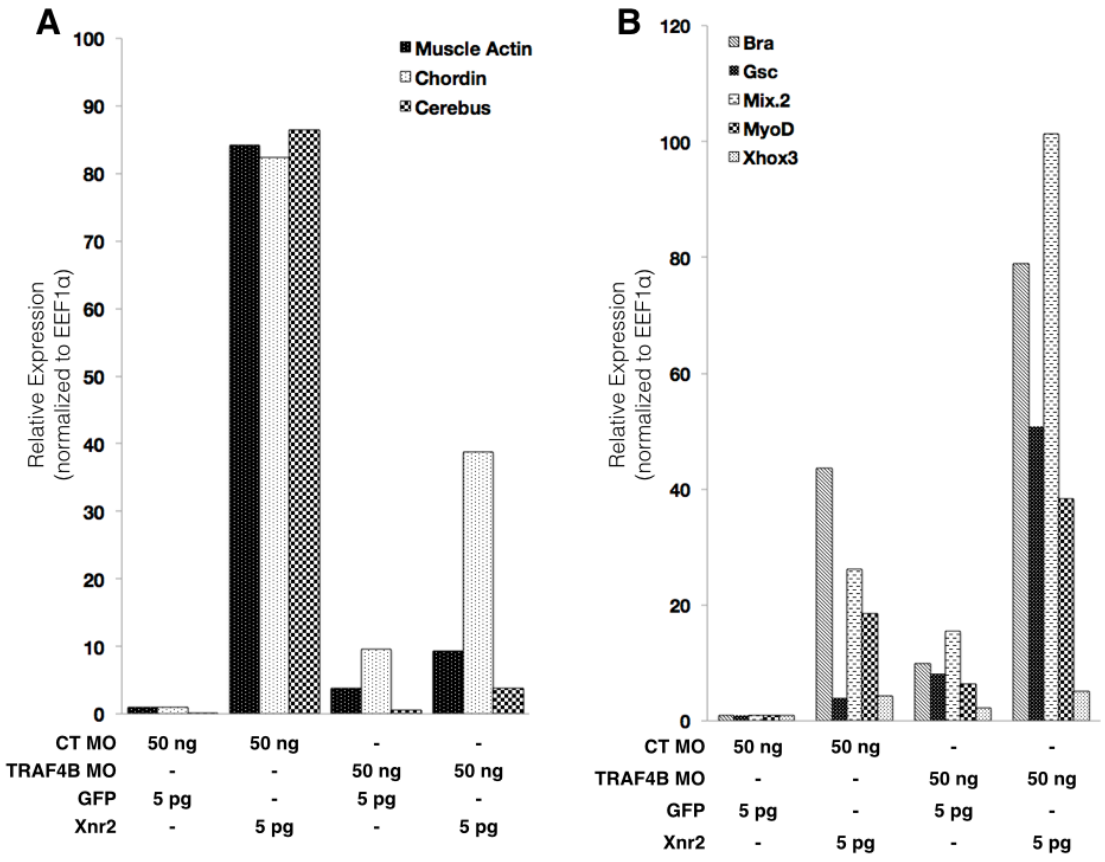

Figure 4.4 | Co-injection of Xnr2 and a TRAF4B MO on mesoderm marker expression. Embryos were injected as written in the animal pole at the two-cell stage. Animal caps were isolated at stage 8 and processed for RT-PCR at stage 13. (**A**) Knockdown of TRAF4 ameliorates the effects of Xnr2 overexpression. Animal caps overexpressing Xnr2 express dorsal mesoderm markers at nearly 80-fold higher levels than control caps and co-injection of Xnr2 and a TRAF4B MO greatly reduces marker expression. (**B**) Genes that show an increase in expression when Xnr2 RNA and a TRAF4B MO are co-expressed.

Chapter 5: Methods

5.1 Preparation of Xenopus laevis Embryos

Xenopus laevis has been a favored research tool in developmental biology due to their simple husbandry, are easily ovulated, produce hundreds of eggs per lay. Embryos are easily produced through in vitro fertilization and develop in a mild salt buffer (MMR) in glassware at room temperature. The embryos themselves are advantageous due to their reproducible fate map that is determined at the time of sperm entry, in addition to their large size and ability to survive manipulation. Adult Female *Xenopus laevis* were injected with 400 – 500 ul of human chorionic gonadotropin into the dorsal lymph sac 14 to 20 hours prior to microinjections. Preparation of embryos and testis were performed according to published methods (Guille, 2007). Minced testes were diluted in 0.1x MMR prior to in vitro fertilization. Embryos were grown and washed with 0.1X MMR.

5.2 Microinjection of Xenopus laevis Embryos

Microinjection of *Xenopus laevis* embryos allows for the study of cellular differentiation and signaling pathways. Signaling ligands, truncated proteins, cellular pathway factors and translation blocking morpholinos, amongst other reagents, may be injected into the embryo and their effects can be viewed on cellular differentiation and development. This dissertation used microinjection of *Xenopus laevis* embryos to introduce either translation blocking morpholinos or RNA encoding ligands that activate TGFβ signaling into the embryo and into tissues where the effects of these reagents may be readily studied.

Embryos were prepared as stated above and microinjections were performed according to (Guille, 2007). Needles were calibrated to either 5nl or 7.5 nl per one injection, and the microinjector (medical systems corporation) average injection conditions were 8.0 psi and 10 milliseconds injection time, although this may vary with each needle.

5.3 Xenopus animal cap assay

The ability of the animal cap to respond to exogenous signaling factors has made the animal cap a model system for induction and differentiation of the ectoderm and mesoderm. The versatility of the animal cap assay is that the cap can respond to growth factors, cell surface receptors and even isolated tissues since it is not yet committed to its epidermal fate. RNA for signaling proteins or translation blocking morpholino oligonucleotides (MO) may be injected into early blastomeres of the two-cell stage or four-cell stage embryos and incubated in 0.1x MMR at room temperature. Animal caps were isolated and cared for as described by Jeremy Green (Green, 1999). Animal caps were then incubated in 0.5x MMR from 18˚C to 24˚C depending on the desired stage.

5.4 Isolating RNA from Xenopus leaves embryonic tissue

Microcentrifuge tubes containing animal caps or whole embryos were stored at -80˚C. When the tissue was ready to be processed for RT-PCR, the microcentrifuge tubes were removed from the -80˚C freezer and placed on ice. Tissue was lysed using a solution of 1ug/ul of RNA grade proteinase K, (Invitrogen, Catalog number: AM2548), was added to 1.5 ml micro centrifuge tubes containing caps or whole embryos. The tubes were vortexed until there were no visible pieces of tissue and incubated at 42˚C for at least 30 minutes. 10 ul of 5M ammonium acetate was added to improve DNA removal by lowering the pH to below 7.0. 500 ul of phenol/chloroform/isoamyl alcohol (Roche, product number 03117987001) was added into each tube, the tubes were shaken then centrifugated at 13,000 rpm for 10 minutes at 4˚C. The aqueous layer was transferred to a clean tube and the wash through centrifugation was repeated once more with phenol/chloroform/isoamyl chloroform, then again with chloroform alone. The aqueous layer was again transferred to a new tube and 2.5 volumes of 100% isopropyl alcohol were added and the tubes mixed. The tubes were incubated at room temperature for 10 min and then centrifugated at 13,000 RPM for 10 minutes. The RNA was collected at the bottom of the tube and the isopropyl alcohol was replaced with 70% ethyl alcohol. The tubes were vortexed to remove the pellet from the bottom, and then the tubes were again centrifugated at 13,000 RPM for 10 minutes. The ethyl alcohol was then removed and the RNA was treated with DNaseI I according to the DNaseI I version 3 manual by Roche (DNaseI I recombinant,

RNase-Free, product number 04716728001). The RNA was then phenol/chloroform extracted as stated above and tested for structural integrity on a 1% bleach gel (Aranda et al., 2012) and the concentration was determined using a Thermo Scientific nanodrop ND-1000 spectrophotometer according to the manual, version 3.7, 2008. RNA samples were stored in RNase-free water at -80˚C.

5.5 Real Time Polymerase Chain Reaction (RT-PCR)

Real-time polymerase chain reaction was used in this study to compare the relative levels of expressed RNA between samples. In every case, each sample was tested for genes of experimental interest and a housekeeping gene, either ornithine decarboxylase (ODC) or Eukaryotic Translation Elongation Factor 1 alpha (eEF1α). Raw fluorescence data was normalized to a housekeeping gene in order to account for differences in initial cDNA concentrations.

cDNA was synthesized from randomly primed total RNA according to the Invitrogen by Life Technologies Superscript II manual, 2010. The presence of cDNA was confirmed in a 30 cycle PCR using an MJ Mini Personal Thermal Cycler from Bio-Rad using the same cycle settings used in the light cycler as stated in the table below. The PCR product was visualized on a 1% agarose gel. Real-Time PCR was performed on a Roche LightCycler 480 using SYBR Green I Master by Roche for the amplification and detection of cDNA targets. The LightCycler was programmed according to Table 5.1, which is adapted from the SYBR Green I Master manual, version 12.

Raw fluorescence data was removed from the LightCycler 480 as a text file and processed using LinReg PCR (Ruijter et al., 2009b). LinReg PCR is a program that determines the baseline and amplification efficiency of each sample, which removes inconsistencies that occur when using the default software of most RT-PCR apparatuses (Ruijter et al., 2009a). LinReg PCR processed data was exported to excel where technical replicates that differed by greater than one cycle were eliminated. The remaining replicates were then averaged and normalized through division by a housekeeping gene. The fluorescence data was then processed again to set a control group, either whole embryos or uninjected animal caps, to 1, allowing the y-axis to easily visualize fold-change differences in gene expression.

Target ˚C	Acquisition Mode	Hold (mm:ss)	Ramp Rate (˚C per sec)	Acquisitions per ˚C
Preincubation				
95	None	10:00	4.4	N/A
Amplification				
95	None	00:10	4.8	N/A
55	None	00:10	2.0	N/A
72	Single	00:15	4.8	N/A
Melting Curve				
95	None	00:05	4.8	N/A
65	None	01:00	2.5	N/A
97	Continuous	N/A	0.11	5
Cooling				
40	None	00:10	2	N/A

N/A = not applicable

Light cycler settings are adapted from recommendations by the SYBR Green I manual by Roche.

Table 5.1 | Roche LightCycler 480 cycle protocol.

Gene	Forward Primer 5' to 3'	Reverse Primer 5' to 3'
BMP4	AGCTCACCAACGAGATGATCG	AACCGTATACATTGCATTGGGAT
Cerberus	AAGAGGAGCACGTAGGAGCAAG	GCCAAAATCACCATGCCC
Chordin	AACTGCCAGGACTGGATGGT	GGCAGGATTTAGAGTTGCTTC
eEF1α	AGGCTCCTTCAAGTATGCCT	ATGCTCACGGGTTTGT CCAT
Epidermal Keratin	CACCAGAACACAGAGTAC	CAACCTTCCCATCAACCA
Goosecoid	GATGCCGCCAGTGCCTC	TGCAGCTCAGTTCGTGACAAA
Mix.2	TGCAAGCCATCATTATTCTAGC	AGGAACCTCTGCCTCGAGACAT
Muscle Actin	GCTGACAGAATGCAGAAG	TTGCTTGGAGGAGTGTGT
MyoD	GGACTCAGATGCCTCAAGCC	TGCTGTCGTAGCTGTTCCTTCTC
NCAM	CACAGTTCCACCAAATGC	GGAATCAAGCGGTACAGA
ODC	CAAAGCTTGTTCTACGCATAGCA	GGTGGCACCAAATTTCACACT
Sox2	CCAGTCCACCTGTAGTCACCTCT	CACTTCTGCCCCAGGTAGGTAC
TRAF4A	CTCTGTTCGAACTAGAAATTTGCTC	GCTGCTCAGATTTCTGTTTTAGG
TRAF4B	CCGTTTGAACTTTGCTCTATG	GACTTTGTATAATGCAAGAGGCTCC
XAG-1	TTGAACCAGACCTGGACT	CTGACTGTCCGATCAGAC

Table 5.2 | Table of LightCycler primers. The LightCycler primers listed were run according to table 5.1.

5.6 mRNA probe synthesis and whole mount in situ hybridization

A 3'UTR TRAF4B probe was created by first downloading and choosing a section of the published NCBI sequence (Fig. 2.1A). Primers were created for the desired 3'UTR region (F-CTGCAGATGGTATGGATGCTC; R-GGTTGCCTCCAACACAAC) and the cloned sequence was subcloned into a pGEM-T plasmid (Promega). mRNA probes were synthesized using a DIG labeling kit (SP6/T7), by Roche. In situ hybridization was performed on MEMFA-fixed embryos as previously described (Kalkan et al., 2009).

5.7 Western Blot

The presence of pSmad1 and total Smad1 was visualized through a western blot. Whole embryos were lysed at Stage 12, and immediately processed for the western blot procedure. Embryos were lysed in a NP-40 lysis buffer solution (20 mM Tris-Cl, pH 8.0; 137 mM NaCl; 10% Glycerol). 1% NP-40, protease inhibitor and phosphatase inhibitor was added immediately prior to use. The embryos were crushed and centrifugated at 4˚C for ten minutes. The clear layer was moved to a new tube without taking the white fatty layer. Centrifugation was repeated until the supernatant became clear. Samples were kept immediately separated by using 10% Tris-Glycine SDS-Polyacrylamide gel electrophoresis (20 min at 60V until the loading dye passes through the stacking gel, then 120V until the loading dye reaches the bottom of the gel). Proteins were transferred to a nitrocellulose membrane at 24V for 60 minutes.

The membrane was blocked according to Cell Signaling suggested blocking solution for pSmad1 (1X TBS, 0.1% Tween-20, 5% w/v BSA). The primary antibody, (cell signaling technology pSmad1/5 (Ser463/465)(41D10) Rabbit mAb, product #9516) was diluted 1:1000 in 1X TBS, 0.1% Tween-20 with 5% BSA. The secondary antibody was blocked in 5% casein in 1X TBS. Fluorescence was measured on an Li-Cor Odyssey fluorescent scanner. Quantifications of blot fluorescence were made using the Odyssey software.

5.8 Nucleotide and Protein Alignments

Alignments were created using Geneious software version 8.1. Sequences were downloaded from the NCBI nucleotide and protein databases. Their respective accession numbers are listed in table 5.2.

Gene	Species	NCBI Accession Number
TRAF1	Homo sapiens	BC024145.2
TRAF2	Homo sapiens	NM_021138.3
TRAF3	Homo sapiens	NM_003300.3
TRAF4A	Danio rerio	AAH65969
TRAF4B	Danio rerio	NP_997982
TRAF4	Drosophila melanogaster	AAD34346
TRAF4	Homo sapiens	BC001769
TRAF4	Mus musculus	AAF44757
TRAF4A	*Xenopus laevis*	NM_001094032.1
TRAF4B	*Xenopus laevis*	NM_001093069.1
TRAF4	*Xenopus tropicalis*	NM_001005074.1
TRAF5	Homo sapiens	NM_004619
TRAF6	Homo sapiens	BC031052

Table 5.2| Table of nucleotide and protein sequences. Sequences used in alignments and phylogenic trees were downloaded from the NCBI protein or nucleotide database. The accession number denotes which sequence was used.

References

Agius, E., Oelgeschläger, M., Wessely, O., Kemp, C. and De Robertis, E. M. (2000). Endodermal Nodal-related signals and mesoderm induction in Xenopus. *Development* **127**, 1173–1183.

Alarcón, C., Zaromytidou, A.-I., Xi, Q., Gao, S., Yu, J., Fujisawa, S., Barlas, A., Miller, A. N., Manova-Todorova, K., Macias, M. J., et al. (2009). Nuclear CDKs drive Smad transcriptional activation and turnover in BMP and TGF-beta pathways. *Cell* **139**, 757–769.

Alexandrova, E. and Thomsen, G. (2006). Smurf1 regulates neural patterning and folding in Xenopus embryos by antagonizing the BMP/Smad1 pathway. *Dev Biol*.

Allendorph, G. P., Vale, W. W. and Choe, S. (2006). Structure of the ternary signaling complex of a TGF-beta superfamily member. *Proc Natl Acad Sci USA* **103**, 7643–7648.

Aranda, P. S., LaJoie, D. M. and Jorcyk, C. L. (2012). Bleach gel: A simple agarose gel for analyzing RNA quality. *ELECTROPHORESIS* **33**, 366–369.

Balemans, W. and Van Hul, W. (2002). Extracellular regulation of BMP signaling in vertebrates: a cocktail of modulators. *Dev Biol*.

Beppu, H., Kawabata, M., Hamamoto, T., Chytil, A., Minowa, O., Noda, T. and Miyazono, K. (2000). BMP type II receptor is required for gastrulation and early development of mouse embryos. *Dev Biol* **221**, 249–258.

Deng, L., Wang, C., Spencer, E., Yang, L., Braun, A., You, J., Slaughter, C., Pickart, C. and Chen, Z. J. (2000). Activation of the IkappaB kinase complex by TRAF6 requires a dimeric ubiquitin-conjugating enzyme complex and a unique polyubiquitin chain. *Cell* **103**, 351–361.

Dosch, R., Gawantka, V., Delius, H., Blumenstock, C. and Niehrs, C. (1997). Bmp-4 acts as a morphogen in dorsoventral mesoderm patterning in Xenopus. *Development* **124**, 2325–2334.

Eisen, J. S. and Smith, J. C. (2008). Controlling morpholino experiments: don't stop making antisense. *Development* **135**, 1735–1743.

Faure, S., Lee, M. A., Keller, T., Dijke, ten, P. and Whitman, M. (2000). Endogenous patterns of TGFbeta superfamily signaling during early Xenopus development. *Development* **127**, 2917–2931.

Feng, X.-H. and Derynck, R. (2005). Specificity and versatility in tgf-beta signaling through Smads. *Annu. Rev. Cell. Dev. Biol.* **21**, 659–693.

Glauner, H., Siegmund, D., Motejadded, H., Scheurich, P., Henkler, F., Janssen, O. and Wajant, H. (2002). Intracellular localization and transcriptional regulation of tumor necrosis factor (TNF) receptor-associated factor 4 (TRAF4). *Eur J Biochem* **269**, 4819–4829.

Goldman, D. C., Hackenmiller, R., Nakayama, T., Sopory, S., Wong, C., Kulessa, H. and Christian, J. L. (2006). Mutation of an upstream cleavage site in the BMP4 prodomain leads to tissue-specific loss of activity. *Development* **133**, 1933–1942.

Grech, A., Quinn, R., Srinivasan, D., Badoux, X. and Brink, R. (2000). Complete structural characterisation of the mammalian and Drosophila TRAF genes: implications for TRAF evolution and the role of RING finger splice variants. *Molecular Immunology* **37**, 721–734.

Green, J. (1999). The animal cap assay. *Molecular Methods in Developmental Biology* **127**, 1–14.

Gritsman, K., Talbot, W. and Schier, A. (2000). Nodal signaling patterns the organizer. *Development*.

Grunz, H. and Tacke, L. (1989). Neural differentiation of Xenopus laevis ectoderm takes place after disaggregation and delayed reaggregation without inducer. *Cell Differ. Dev.* **28**, 211–217.

Guille, M. (2007). 10 Microinjection into Xenopus Oocytes and Embryos. *Methods in Molecular Biology, Vol. 127: Molecular Methods in Developmental Biology:*

Xenopus and Zebrafish 111–123.

Gurdon, J. B. and Hopwood, N. (2000). The introduction of Xenopus laevis into developmental biology: of empire, pregnancy testing and ribosomal genes. *The International Journal of Developmental Biology* **44**, 43–50.

Hata, A., Lagna, G., Massagué, J. and Hemmati-Brivanlou, A. (1998). Smad6 inhibits BMP/Smad1 signaling by specifically competing with the Smad4 tumor suppressor. *Genes & Development* **12**, 186–197.

Hellsten, U., Khokha, M. K., Grammer, T. C., Harland, R. M., Richardson, P. and Rokhsar, D. S. (2007). Accelerated gene evolution and subfunctionalization in the pseudotetraploid frog Xenopus laevis. *BMC Biol.* **5**, 31.

Hemmati-Brivanlou, A. and Thomsen, G. H. (1995). Ventral mesodermal patterning in Xenopus embryos: expression patterns and activities of BMP-2 and BMP-4. *Developmental genetics* **17**, 78–89.

Hill, C. S. (2001). TGF-β signalling pathways in early Xenopus development. *Curr Opin Genet Dev* **11**, 533–540.

Kalkan, T., Iwasaki, Y., Park, C. Y. and Thomsen, G. H. (2009). Tumor necrosis factor-receptor-associated factor-4 is a positive regulator of transforming growth factor-beta signaling that affects neural crest formation. *Molecular Biology of the Cell* **20**, 3436–3450.

Kedinger, V. and Rio, M.-C. (2007). Chapter 5 TRAF4, the unique family member. *Advances in experimental medicine and biology* **597**, 60–71.

Khokha, M. K., Yeh, J., Grammer, T. C. and Harland, R. M. (2005). Depletion of three BMP antagonists from Spemann's organizer leads to a catastrophic loss of dorsal structures. *Developmental Cell* **8**, 401–411.

Kingsley, D. M. (1994). The TGF-beta superfamily: new members, new receptors, and new genetic tests of function in different organisms. *Genes & Development* **8**, 133–146.

Kintner, C. R. and Melton, D. A. (1987). Expression of Xenopus N-CAM RNA in ectoderm is an early response to neural induction. *Development* **99**, 311–325.

Kishi, M., Mizuseki, K., Sasai, N., Yamazaki, H., Shiota, K., Nakanishi, S. and Sasai, Y. (2000). Requirement of Sox2-mediated signaling for differentiation of early Xenopus neuroectoderm. *Development* **127**, 791–800.

Kishigami, S. and Mishina, Y. (2005). BMP signaling and early embryonic patterning. *Cytokine and Growth Factor Reviews*.

Krajewska, M., Krajewski, S., Zapata, J. M., Van Arsdale, T., Gascoyne, R. D., Berern, K., McFadden, D., Shabaik, A., Hugh, J., Reynolds, A., et al. (1998). TRAF-4 expression in epithelial progenitor cells. Analysis in normal adult, fetal, and tumor tissues. *Am J Pathol* **152**, 1549–1561.

Kuroda, H., Fuentealba, L., Ikeda, A., Reversade, B. and De Robertis, E. M. (2005). Default neural induction: neuralization of dissociated Xenopus cells is mediated by Ras/MAPK activation. *Genes & Development* **19**, 1022–1027.

Labbé, E., Silvestri, C., Hoodless, P. A., Wrana, J. L. and Attisano, L. (1998). Smad2 and Smad3 positively and negatively regulate TGF beta-dependent transcription through the forkhead DNA-binding protein FAST2. *Molecular Cell* **2**, 109–120.

Lamb, T. M., Knecht, A. K., Smith, W. C., Stachel, S. E., Economides, A. N., Stahl, N., Yancopolous, G. D. and Harland, R. M. (1993). Neural induction by the secreted polypeptide noggin. *Science* **262**, 713–718.

Masson, R., Régnier, C. H., Chenard, M. P., Wendling, C., Mattei, M. G., Tomasetto, C. and Rio, M. C. (1998). Tumor necrosis factor receptor associated factor 4 (TRAF4) expression pattern during mouse development. *Mechanisms of development* **71**, 187–191.

Mignone, F., Gissi, C., Liuni, S. and Pesole, G. (2002). Untranslated regions of mRNAs. *Genome Biol.* **3**, REVIEWS0004.

Moody, S. A. (1987). Fates of the blastomeres of the 32-cell-stage Xenopus embryo. *Dev Biol* **122**, 300–319.

Osada, S. I. and Wright, C. V. (1999). Xenopus nodal-related signaling is essential for mesendodermal patterning during early embryogenesis. *Development* **126**, 3229–3240.

Park, Y. C., Burkitt, V., Villa, A. R., Tong, L. and Wu, H. (1999). Structural basis for self-

association and receptor recognition of human TRAF2. **398**, 533–538.

Piccolo, S., Sasai, Y., Lu, B. and De Robertis, E. M. (1996). Dorsoventral patterning in Xenopus: inhibition of ventral signals by direct binding of chordin to BMP-4. *Cell* **86**, 589–598.

Preiss, A., Johannes, B., Nagel, A. C., Maier, D., Peters, N. and Wajant, H. (2001). Dynamic expression of Drosophila TRAF1 during embryogenesis and larval development. *Mechanisms of development* **100**, 109–113.

Rothe, M., Wong, S. C., Henzel, W. J. and Goeddel, D. V. (1994). A novel family of putative signal transducers associated with the cytoplasmic domain of the 75 kDa tumor necrosis factor receptor. *Cell* **78**, 681–692.

Rousseau, A., McEwen, A. G., Poussin-Courmontagne, P., Rognan, D., Nominé, Y., Rio, M.-C., Tomasetto, C. and Alpy, F. (2013). TRAF4 Is a Novel Phosphoinositide-Binding Protein Modulating Tight Junctions and Favoring Cell Migration. *PLoS Biol* **11**, e1001726.

Rousseau, A., Rio, M.-C. and Alpy, F. (2011). TRAF4, at the Crossroad between Morphogenesis and Cancer. *Cancers (Basel)* **3**, 2734–2749.

Ruijter, J. M., Ramakers, C., Hoogaars, W. M. H., Karlen, Y., Bakker, O., van den Hoff, M. J. B. and Moorman, A. F. M. (2009a). Amplification efficiency: linking baseline and bias in the analysis of quantitative PCR data. *Nucleic Acids Research* **37**, e45–e45.

Ruijter, J. M., van der Velden, S. and Ilgun, A. (2009b). LinRegPCR (11.0) Manual. *Heart Failure Research Center Academic Medical Center Amsterdam, the Netherlands* 1–29.

Sasai, Y., Lu, B., Steinbeisser, H. and De Robertis, E. M. (1995). Regulation of neural induction by the Chd and Bmp-4 antagonistic patterning signals in Xenopus. **376**, 333–336.

Sato, S. M. and Sargent, T. D. (1989). Development of neural inducing capacity in dissociated Xenopus embryos. *Dev Biol* **134**, 263–266.

Shi, Y. and Massagué, J. (2003). Mechanisms of TGF-beta signaling from cell membrane to the nucleus. *Cell* **113**, 685–700.

Shiels, H., Li, X., Schumacker, P. T., Maltepe, E., Padrid, P. A., Sperling, A., Thompson, C. B. and Lindsten, T. (2000). TRAF4 deficiency leads to tracheal malformation with resulting alterations in air flow to the lungs. *Am J Pathol* **157**, 679–688.

Summerton, J. and Weller, D. (1997). Morpholino antisense oligomers: design, preparation, and properties. *Antisense Nucleic Acid Drug Dev* **7**, 187–195.

Takeuchi, M., Rothe, M. and Goeddel, D. V. (1996). Anatomy of TRAF2. Distinct domains for nuclear factor-kappaB activation and association with tumor necrosis factor signaling proteins. *J. Biol. Chem.* **271**, 19935–19942.

Uno, Y., Nishida, C., Takagi, C., Ueno, N. and Matsuda, Y. (2013). Homoeologous chromosomes of Xenopus laevis are highly conserved after whole-genome duplication. *Heredity (Edinb)* **111**, 430–436.

Wang, W., Mariani, F. V., Harland, R. M. and Luo, K. (2000). Ski represses bone morphogenic protein signaling in Xenopus and mammalian cells. *Proc Natl Acad Sci USA* **97**, 14394–14399.

Wills, A. E., Choi, V. M., Bennett, M. J., Khokha, M. K. and Harland, R. M. (2010). BMP antagonists and FGF signaling contribute to different domains of the neural plate in Xenopus. *Dev Biol* **337**, 335–350.

Wilson, P. A. and Hemmati-Brivanlou, A. (1995). Induction of epidermis and inhibition of neural fate by Bmp-4. **376**, 331–333.

Wrana, J. L., Attisano, L., Wieser, R., Ventura, F. and Massagué, J. (1994). Mechanism of activation of the TGF-beta receptor. **370**, 341–347.

Xie, P. (2013). TRAF molecules in cell signaling and in human diseases. *J Mol Signal* **8**, 7.

Zapata, J. M., Martinez-Garcia, V. and Lefebvre, S. (2007). Chapter 1 Phytogeny of the TRAF/MATH Domain. *TNF Receptor Associated Factors (TRA* 1–24.

Zhang, L., Zhou, F., de Vinuesa, A. G., de Kruijf, E. M., Mesker, W. E., Hui, L., Drabsch, Y., Li, Y., Bauer, A., Rousseau, A., et al. (2013). TRAF4 Promotes TGF-b Receptor Signaling and Drives Breast Cancer Metastasis. *Molecular Cell* **51**, 559–572.

Zhou, A. Y., Shen, R. R., Kim, E., Lock, Y. J., Xu, M., Chen, Z. J. and Hahn, W. C. (2013). IKKε-mediated tumorigenesis requires K63-linked polyubiquitination by a cIAP1/cIAP2/TRAF2 E3 ubiquitin ligase complex. *CellReports* **3**, 724–733.

Zhu, H., Kavsak, P., Abdollah, S., Wrana, J. L. and Thomsen, G. H. (1999). A SMAD ubiquitin ligase targets the BMP pathway and affects embryonic pattern formation. **400**, 687–693.

Zimmerman, L. B., De Jesús-Escobar, J. M. and Harland, R. M. (1996). The Spemann organizer signal noggin binds and inactivates bone morphogenetic protein 4. *Cell* **86**, 599–606.